MODELING OF AGGREGATION AND RIMING IN OROGRAPHIC CLOUDS OVER THE NORTHERN COLORADO ROCKIES

ELIZABETH A. MULVIHILL

Colorado State University

DEPARTMENT OF ATMOSPHERIC SCIENCE

PAPER NO. 463

MODELING OF AGGREGATION AND RIMING IN OROGRAPHIC CLOUDS OVER THE NORTHERN COLORADO ROCKIES

By

Elizabeth A. Mulvihill

This report was prepared with support provided by National Science Foundation Grants ATM-8407543, ATM-8519370, ATM-8704776, ATM-8813345
Principal Investigator Lewis O. Grant

Department of Atmospheric Science
Colorado State University
Fort Collins, Colorado

May 1990

Atmospheric Science Paper

ABSTRACT OF THESIS

MODELING OF AGGREGATION AND RIMING IN OROGRAPHIC CLOUDS OVER THE NORTHERN COLORADO ROCKIES

This thesis addresses problems arising in the modeling of aggregation and riming in mesoscale cloud models. Two case studies are used to test these portions of the microphysical parameterization in the Colorado State University Regional Atmospheric Modeling System.

The cases modeled were taken from the Colorado Orographic Seeding Experiments. Each case was dominated by a particular precipitation formation mechanism. This allowed for the separate testing of the riming and aggregation parameterizations. The portions of the storms modeled were documented in great detail with ground and aircraft observations.

The modeling portion of this study involved control simulations as well as several experiments geared to correct deficiencies identified using the controls. The main conclusions are as follows.

The model has difficulty predicting the presence of cloud water in areas observed in the field. The vertical distribution of the concentration of ice crystals predicted contradicts observed distributions. Also, the amount of graupel predicted by the model did not mirror observed precipitation characteristics.

From the experiments conducted suggestions can be made for improvements to the model's microphysical parameterization. The graupel

density currently used should be lowered. The value of 0.2 g/cm^3 seemed to work best for the case examined. Also, the addition of the dependency of crystal concentration on air density brought predicted concentrations closer to those observed but had no effect on the vertical distribution problem. An exploratory sensitivity test showed that the introduction of longwave radiation into the model should be further investigated.

Elizabeth A. Mulvihill
Department of Atmospheric Science
Colorado State University
Fort Collins, Colorado 80523
Spring 1990

ACKNOWLEDGEMENTS

So many people have contributed to the completion of this thesis. First, I would like to thank my advisor, Prof. Lewis Grant, for his guidance and perseverance with my research. His encouragement to present conference papers and contribute to a journal article enhanced my graduate education.

Prof. William Cotton was a valuable member of my graduate committee. His unique methods of motivation helped me see this project through to the end. Prof. Paul Mielke also served on my committee and contributed ideas for my research method.

Most of this work would not be possible without the help of Dr. Gregory Tripoli. His patience in helping me decipher both the RAMS and the NCAR computing system was extraordinary. Dr. Robert Rauber helped me piece together the field data of the case studies used in the simulations.

Ms. Lucy McCall is responsible for many of the figures appearing in my thesis. Ms. Jan Davis helped in preparing the final form of the text. The final version of this thesis would not be possible without the assistance of Ms. Glenda Snavely, Sgt. James Lavin and Tsgt. Frank Henry in finding word processing facilities for me to use.

Finally, I would like to thank those who gave me moral support. My many close friends, especially Mr. David Changnon. My mother, who has been a strong motivational force all my life, and my father who has given

me great professional guidance and encouragement. And Sgt. Daniel Page, my fiance, whose support and patience is priceless.

The support of the National Science Foundation which provided the funding for this research is gratefully acknowledged.

TABLE OF CONTENTS

LIST OF FIGURES

Chapter 1. INTRODUCTION

Aggregation of ice crystals and riming of water droplets by ice crystals are important mechanisms in the formation of precipitation. Both are very effective in transferring water mass from clouds to the ground. These mechanisms are present in both stable and convective clouds and contribute to the formation of rain, snow and hail.

Many studies have outlined the role of these two processes in precipitation development. Hosler et al. (1957) identified aggregation as contributing significantly to precipitation growth in the middle and high latitudes. Melted aggregates were observed to initiate larger raindrops than those formed by single crystals (Hosler and Hallgren, 1960). Aggregation also plays an important role in the formation of snowflakes (Passarelli and Srivastava, 1979). More recently, aggregation and riming working together have been credited in the formation of hail (Heymsfield, 1982). Cotton et al. (1982) attributed a deficiency in the precipitation amount predicted by their numerical model to the absence of an aggregation parameterization.

Similarly, riming is an efficient mechanism in precipitation development. Studies have shown that riming increases the snowfall rate (Heymsfield, 1967 and Hobbs et al., 1971) as well as the density of precipitation (Power et al., 1964; Jiusto and Kaplan, 1972). Rauber (1985) stated that rimed crystals have steeper trajectories since they fall faster than unrimed crystals. Therefore, riming can alter the

distribution of snowfall in a watershed. Heavy riming results in the formation of graupel (Holroyd, 1964; Knight and Knight, 1973; Reinking, 1973) which have been identified as hail embryos (Knight and Knight, 1970).

Because of the importance of these mechanisms in the formation of precipitation, numerical models must simulate them correctly. Difficulties in model development arise with the limitations in the computing memory and the time requirements of a detailed microphysical model. A compromise between accuracy and computing requirements is necessary for the best possible representation.

The predictive capabilities of a parameterization are best tested against well documented cloud systems studied in the field. Such case studies are used in the development of numerical models. Modifications are made until the parameterization accurately predicts the field observations. This process yields a model specific to one case rather than universal. Additional cases with a variety of precipitation characteristics should be used to further test the model. General deficiencies can then be identified, and a more universal representation can be developed.

In this study, the Colorado State University Regional Atmospheric Modeling System (CSU RAMS) was used to simulate mesoscale orographic cloud systems in two dimensions. Though originally developed to simulate convective clouds, CSU RAMS has since been adapted for orographic cases. Testing and refining this model was simplified in these more stable clouds because of the relatively steady state they obtain.

A detailed data set, collected during the Colorado Orographic Seeding Experiments (COSE), was used for these tests. The COSE were

conducted in the Yampa Valley on the western slope of the Colorado Rockies near Steamboat Springs, CO. Two case studies from COSE were used. One in which aggregation dominated in the formation of precipitation and the other in which riming dominated.

Numerical simulations of the two cases were conducted by initializing the model with field data and allowing the airflow to achieve a steady state before activating the microphysical simulation. Model predictions were then compared to the field observations with respect to microphysical characteristics.

From these results several sensitivity tests have been developed to test the representation of aggregation and riming in the model and to explore possible improvements. Each test was compared with the control simulations. From these comparisons suggestions were made for model improvements.

Chapter 2. BACKGROUND

This chapter gives a background of previous work in the areas of aggregation and riming. Only topics which relate directly to the research performed for this thesis are presented. Included are the structure of clouds in which riming occurs, the size spectra of collected droplets and the minimum crystal size necessary for riming to occur. Since all ice crystals are predicted by RAMS as hexagonal plates, the microphysical theories addressed are done so with respect to these types of crystals.

2.1 Growth by Riming

The structure of the clouds in which riming occurs was first examined. Since riming takes place only in the presence of liquid water, Rauber (1985) identified three major areas of liquid water in northern Colorado orographic clouds. Supercooled liquid water appeared near the top of the cloud, in the area of greatest orographic lift and in the lower regions of the cloud near the cloud base. Hobbs et al. (1971) found that in pre-frontal cloud systems riming was evident near the crest of the Cascade Mountains. They believed riming occurred between the ground and 5000 feet AGL. Riming was more common and graupel particles were seen in transitional and post frontal conditions. These conditions produced orographic clouds with embedded convective elements. In his study in the Sierra-Nevadas, Reinking (1975, 1979) described the primary areas where

riming occurred as convective cells which produced liquid water. He found convection embedded in stratiform clouds as frontal systems which moved through the area were enhanced by upper level troughs. Also, post frontal and post trough systems contained more shallow convection because of the capping effects of subsidence aloft. Reinking concluded that convection and therefore riming occurred in all phases of snowstorms in the Sierra-Nevadas.

The size spectra of droplets collected has been another area of interest. In general, the size of the most commonly collected droplets increased with the size of the crystal (Hariyama, 1975). The size spectra of these droplets broadened as the size of the crystal increased (Wilkins and Auer, 1970). The data analyzed by Wilkins and Auer (1970) contained a large proportion of hexagonal plates. In the COSE area, Borys et al. (1987) observed rime on crystals only in the presence of cloud droplets greater than 10 μm in dianeter. The minimum droplet size collected by hexagonal plates was determined to be 10 μm in diameter by Wilkins and Auer (1970) and Hariyama (1975) while Reinking (1973) and D'Errico and Auer (1978) reported values of 5 μm in diameter for hexagonal plates. The most efficiently collected droplet was found to be 15 μm in diameter by D'Errico and Auer (1978) and by Pitter (1977) on smaller hexagonal plates. It should be noted that Reinking observed that hexagonal plates did not collect significant amounts of rime and rarely formed graupel.

The minimum crystal dimension required for the onset of riming has been addressed by several people. Reinking (1979) found that hexagonal plates grew to between 150 μm and 200 μm in Sierra Nevada cloud systems before riming was observed. He compared his results with previous studies and attempted to explain the discrepancies. Hariyama (1975) analyzed a

large sample of crystals observed over a ten year period in Sapporo, Japan to determine that 150 μm was the minimum dimension for hexagonal plates. A smaller data set used by Wilkins and Auer (1970) produced a value of approximately 200 μm in the Laramie Range of Wyoming, but a later study by D'Errico and Auer (1978) conducted in the same area yielded a value of 140 μm as a minimum dimension. An early study by Ono (1969) used a small data set to give a rather high value of 300 μm in southeastern Australia. Reinking (1979) pointed out that many crystals grow "well beyond" their critical size before riming commences due to the competition between crystals for cloud water, the nonuniform distribution of cloud water and the stochastic nature of riming.

2.2 Aggregation

A detailed review of current theories in aggregation was given by Rauber (1985) in his doctorate dissertation. The background of aggregation here has been extracted from his work and expanded upon in some areas. Five different mechanisms have been used to explain the process of aggregation. Hosler and Hallgren (1960) believed that ice particles had a thin outer layer of liquid water which froze on contact with another particle. Fletcher (1968) theoretically supported this idea. Sintering, the formation of ice bonds through the transport of water molecules to the point of contact of two ice crystals, was suggested by Hobbs and Mason (1964). Electrical attraction has also been credited in the aggregation process by Smith-Johannsen (1965,1969), Odencranz et al. (1968), Magono and Tazawa (1972) and Latham and Saunders (1970). Mechanical interlocking of ice crystals with branched structures has been

described by Ohtake (1969), Rogers (1974) and Jiusto and Weickmann (1973). Aggregation may also be enhanced by supercooled water (Rauber, 1985) in that riming acts to "cement" aggregates. The dependence of aggregation on crystal concentration has been investigated by Jiusto (1971) and Hobbs et al. (1974). The rate of aggregation increased as crystal concentration increased. Also, it has been observed and theoretically determined that particles of contrasting sizes and habits are more likely to aggregate. (Rogers, 1974; Hobbs et al., 1974; Jiusto and Weickmann, 1973; and Passarelli and Srivastava, 1979).

Rauber (1985) found that certain crystal habits dominated the larger aggregates and thus had larger collection efficiencies in the northern Colorado Rockies. Most of the larger aggregates observed contained planar and spatial dendrites.

2.3 Numerical modeling of Riming and Aggregation

The last area to explore is the numerical modeling of aggregation and riming. Representations of these two processes have been based on both theoretical and experimental work.

Numerical representations are developed by breaking these two precipitation mechanisms into distinct steps. The collection of ice crystals by another ice crystal constitutes aggregation. Once one ice crystal is collected, these two ice crystals become an aggregate. Aggregates also collect ice crystals. So, the aggregation process can be broken into three steps: the collection of ice crystals by an individual ice crystal, the simultaneous conversion of an ice crystal to an aggregate and the collection of ice crystals by aggregates.

Riming, on the other hand, is more complicated. Supercooled water droplets can be collected by individual ice crystals, aggregates and graupel particles. Heavy riming of ice crystals and aggregates can yield graupel and then hail. Supercooled drizzle drops and raindrops can freeze and serve as embryos for graupel particles and hailstones. In this study of orographic cloud microphysics, the development of hail will be ignored. Thus the riming process will be divided into five parts: the collection of supercooled cloud droplets by ice crystals, aggregates and graupel and the conversion of ice crystals and aggregates to graupel particles.

There have been several approaches to parameterize these mechanisms. Young (1974a) introduced a multi-level microphysical model to simulate orographic clouds (Young, 1974b). He developed a very intricate microphysical model in which ice crystals are divided according to size. Riming is modeled as a discrete collection process by calculating the number of drops collected by an ice crystal using the equation

$$\Delta N_j = A\ N_{k,m}\ N_j\ \left|V_{t,k,m} - V_{t,j}\right|\ E_{k,m,j}\ \Delta t \qquad (1)$$

where N is the number of particles denoted as water drops by the subscript j and as ice crystals by the subscripts k,m. Cross sectional area is represented by A. v_t is the terminal velocity and E is the collection efficiency of water drops by ice crystals. The time step over which the number of drops collected is calculated is given by Δt. Aggregation is modeled in a similar way. Young broke the collection equation in two to allow for collisions between particles of similar fall velocities and those with large differences in fall velocities. For large differences in fall velocity, the number of particles of radius r_j collected is

$$\Delta N_j = \pi \; N_j \; N_k \; (r_k + r_j)^2 \; \left| V_{t,k} - V_{t,j} \right| \; \Delta t \qquad (2)$$

where the subscript j denotes the particle collected and k denotes the collector. When there is a relatively small difference in fall velocities, the number of particles collected is calculated using a collision rate developed by Sasyo (1971). The difference between fall velocities is determined to be small when less than

$$\tfrac{1}{2} \; \pi^{-1/2} (V_{t,k} + V_{t,j}) \qquad (3)$$

and the number of collected particles is given by

$$\Delta N_j = \tfrac{1}{2} \; \pi^{1/2} \; N_j \; N_k \; (r_k + r_j)^2 \; (V_{t,k} + V_{t,j}) \; \Delta t \qquad (4)$$

where the variables are identical to those in the previous collection equation. Using a continuous bin technique, Young then predicted the size spectra of liquid drops, ice crystals, graupel particles and aggregates.

Hobbs et al. (1973) developed a Lagrangian microphysical model which calculates the growth of ice particles as they travel through orographic clouds. Potential precipitation particles are allowed to grow by vapor deposition, aggregation and riming. The microphysical structure of the cloud is not affected by the particles traveling through it. This model was used to compare the effects of the different growth mechanisms on particle trajectories and masses.

Calculations of the mass growth rate due to riming and aggregation are made by assuming continuous accretion of ambient cloud droplets by ice particles settling through the cloud. The equation for riming is

$$\left(\frac{dM}{dt}\right)_{rim} = A\ (V_c - V_d)\ E_d\ X \tag{5}$$

where A is the cross-sectional area, v_c and v_d are the fall velocities of ice particles and cloud droplets respectively, E_d is the collection efficiency of an ice particle for cloud droplets and X is the mass of condensation products per unit volume of air. Aggregation is represented by a continuous accretion equation similar to that for riming given by

$$\left(\frac{dM}{dt}\right)_{agg} = \pi\ r^2\ (V_c - V_a)\ E_a\ X \tag{6}$$

where r is the effective radius of an aggregate at time t. The other variables are defined similarly to the previous equation in that v_a is the fall velocity of an aggregate and E_a is the collection efficiency of an aggregate for ambient ice particles.

The last model reviewed is that developed at the South Dakota School of Mines under the direction of H. Orville. The ice phase representation has been discussed by Chang (1977) and Lin et al. (1983). This two-dimensional model has been used in the simulation of hail producing convective storms.

Hydrometeors are broken into precipitation size particles (snow, hail and rain) and those with negligible terminal velocities (cloud water and cloud ice). These are predicted in terms of mixing ratios. Snow is predicted as hexagonal graupel with an exponential size distribution.

Chang (1977) represented the riming growth of one snow particle by the continuous accretion equation

$$\left.\frac{dM_s}{dt}\right]_{ACW} = E_{SW}\ \rho\ l_{CW}\ u_{D_s}\ \pi\ \frac{D_s^2}{4} \tag{7}$$

where E_{SW} is the collection of water by snow, ρ is the air density, l_{CW} is the mixing ratio of cloud water and u_{Ds} is the terminal velocity for snow of diameter D_s. Again, aggregation was given a similar representation defined as

$$\left.\frac{dM_s}{dt}\right]_{ACI} = E_{SI}\ \rho\ X_{CI}\ u_{DS}\ \pi\ \frac{D_s^2}{4} \tag{8}$$

where X_{CI} is the cloud ice mixing ratio and the other terms are similar to the above equation.

These equations are integrated over an assumed size distribution of snow particles and are used in calculating the total production of snow.

These three models show different ways of approaching the representation of riming and aggregation in numerical models. They have been developed to simulate various types of situations and thus differ accordingly. The general concepts were presented to give a background before the numerical model used in this study is described.

Chapter 4. COSE FIELD OBSERVATIONS

The field data used to test the ability of RAMS to simulate orographic clouds was collected during the third Colorado Orographic Seeding Experiment (COSE) which took place from December 1981 to January 1982 near Steamboat Springs, Colorado in the Yampa Valley. The instrumentation used during this project has been thoroughly described by Uttal (1985) and Rauber (1985). A brief summary is presented in this chapter.

The purpose of COSE was to characterize orographic clouds over the northern Colorado Rockies and their microphysical characteristics. The Steamboat Springs area was chosen because of the relatively flat upwind fetch of the Park Range. Thus, the main orographic influence on clouds which form in this area is the Park Range.

4.1 Ground Observations

i. Dual-Channel Microwave Radiometer

This instrument, developed by the National Oceanic and Atmospheric Administration (NOAA) measures total liquid water and water vapor in a cloud system integrated along a column of air determined by the orientation of the antenna beam. The antenna rotates with respect to

The nucleation of ice crystals by deposition/sorption is determined using a modified version of the formula developed by Fletcher (1962). This version includes a supersaturation dependency developed by Huffman and Vali (1973). The effect was to suppress the production of crystals in regions which are relatively dry. The equation for the concentration of ice crystals is given by

$$N_i^* = N_{io}\, e^{\beta_2 T_s}\, 3.15\, \left[(S_i - 1)\times 100\right]^{4.5} \tag{9}$$

where $N_{io} = 10^{-2}$ m^{-3}, $T_s = 273.16 - T$, and $(S_i - 1)$ is the supersaturation with respect to ice.

The collection equations for the different types of ice particles are derived from the same basic equation for the rate of change of the mass of an ice particle due to the collection of cloud droplets given by

$$\left.\frac{dm}{dt}\right]_{CL} = \frac{\pi D^2}{4}\, |V - V_c|\, E\, \rho_o\, r_c \tag{10}$$

In equation (10) D is the diameter of the ice particle, v is the terminal velocity of the ice particle, and v_c is the terminal velocity of a cloud droplet which is assumed insignificant. The collection efficiency E is constant, ρ_o is the air density and r_c is the mixing ratio of cloud water. The actual collection equations used in the model are calculated for a population of ice particles at a particular grid point using

$$CL = \int_o^\infty \frac{1}{\rho_o} \left.\frac{dm}{dt}\right]_{CL} N(D)\, dD \tag{11}$$

where N(D) is the number of ice particles of diameter D given by the Marshall-Palmer equation

$$N(D) = \frac{N_i}{D_m} e^{-D/D_m} \tag{12}$$

where D_m is the characteristic diameter.

3.1 Riming Equations

The current model representation of riming has been thoroughly discussed in Cotton et al. (1982) and Cotton et al. (1986). Riming is activated in the model when ice crystals have achieved a diameter of 200 μm in the presence of 10^{-5} g/g of cloud water. No minimum droplet size is expressly defined to cut off riming. The coalescence efficiency between crystals and cloud droplets is set to unity. In other words, an ice particle collects all cloud droplets with which it collides.

The collection of cloud water by ice crystals is easily derived from

$$CL_{ci} = \frac{\pi}{4} \bar{v}_i \, D_i^2 \, N_i \, \bar{r}_c \, E_{ci} \, h(T_s) \tag{13}$$

where the subscripts c and i denote cloud water and ice crystals, respectively. Average quantities are symbolized by an overbar, and $h(T_s)$ is the heaviside step function. This is equal to 1 if T_s is less than 0°C, and it is equal to 0 if T_s is greater than 0°C. N_i is the concentration of ice crystals at that particular grid point. The collection equations for aggregates and graupel particles differ from the equation for ice

crystals in how the terms for the terminal velocity of the particles and the collection efficiencies for cloud droplets are defined. The fall velocity of aggregates is defined as

$$v_a = \left[\frac{4 g \rho_a}{3 \rho_o C_{D_a}}\right]^{1/2} D_a^{1/2} \tag{14}$$

where g is the acceleration due to gravity, ρ_{ia} is the aggregate density, ρ_o the air density, C_D is the drag coefficient of 1.3 and D_a is the aggregate diameter. The collection efficiency of cloud droplets by aggregates is calculated similarly to the collection efficiency of cloud water by single ice crystals. Substituting the terminal velocity equation and the characteristic diameter of a population of aggregates into Equation (11) yields

$$CL_{ca} = 2.42 \left[\frac{g \rho_o}{C_{D_a} \beta_1}\right]^{1/2} E_{ca} \; D_{m_a}^{-0.2} \; r_a \; r_c \tag{15}$$

The terminal velocity of graupel is found using

$$V_g(D) = \left(\frac{4 \rho_g g}{3 \rho_o C_{D_g}}\right)^{1/2} D_g^{1/2} \tag{16}$$

where ρ_g is the density of graupel (0.6 g/cm^{-3})and C_{Dg}, the drag coefficient of graupel is 0.6. After substitution into Equation (11), the collection equation becomes

$$CL_{cg} = 1.16 \left(\frac{g}{C_{D_g}}\right)^{1/2} \left(\frac{\rho_o}{\rho_g}\right)^{1/3} N_{ig}^{1/6} \tag{17}$$

3.2 Aggregation Equations

Aggregates are initiated by the conversion of ice crystals into aggregates. This equation is given by

$$CN_{ia} = \frac{\pi D_i^2}{6} v_i \bar{E}_i N_i r_i X \tag{18}$$

where X is proportional to the variance in particle fall speed. The estimate of 0.25 by Passarelli and Srivastava (1978) is used in the model.

Aggregates continue to grow through the collection of ice crystals. The collection equation for this process is given by

$$CL_{ia} = \frac{r_i}{N_i} \int_0^\infty K_i N_i N(D_a) dD_a \tag{19}$$

where

$$K_i = \frac{\pi}{4} (D_a + D_i)^2 |v_a - v_i| E_{ia} \tag{20}$$

and

$$\bar{v}_a = 2.49 \beta_1^{0.5} \left[\frac{g}{3\rho_o C_{D_a}}\right]^{1/2} D_{m_a}^{0.2} \tag{21}$$

and the collection equation becomes

$$CL_{ia} = \frac{0.5\rho_o}{\beta_1} E_{ia} |\bar{v}_a - \bar{v}_i| D_{m_a}^{2.4} (C D_{m_a}^2 + 2 D_i D_{m_a} + D_i^2) r_a r_i \tag{22}$$

where β_1=0.015 $gm^{-2.4}$ and D_m=0.33 cm. The collection efficiency of ice by aggregates E_{ia} is calculated with

$$E_{ia} = \min\left[10^{0.035(T_a - 273.16) - 0.7}, 0.2\right] \tag{23}$$

where the temperature of the surface of an aggregate is

$$T_a = T + 0.25\ \rho_w\ \frac{D_{m_a}^{\ 2}}{kr_a}\ (L_{vi}\ V\ D_{va} - L_{il}\ CL_{ca}) \tag{24}$$

Between -12°C and -15°C the collection efficiency is set to 140% to account for enhanced collection between dendritic ice crystals (Rauber, 1985).

The two-dimensional model domain extends in the horizontal for 367 km with 0.718 km grid spacing and in the vertical to 15.5 km with 0.50 km grid spacing. Figure 1 shows a west to east cross section of the COSE topography at 40° 30′ used in the model simulation. The actual topographic representation used for the numerical simulations has been smoothed by averaging in the north to south direction over 4° latitude. A cross sectional cut was then taken at 39° latitude to give the best possible two-dimensional representation of the COSE area (see figure 2).

The time step used was dependent on the wind speeds and the stability of the initiating sounding. Several adjustments were necessary to obtain the largest time step possible.

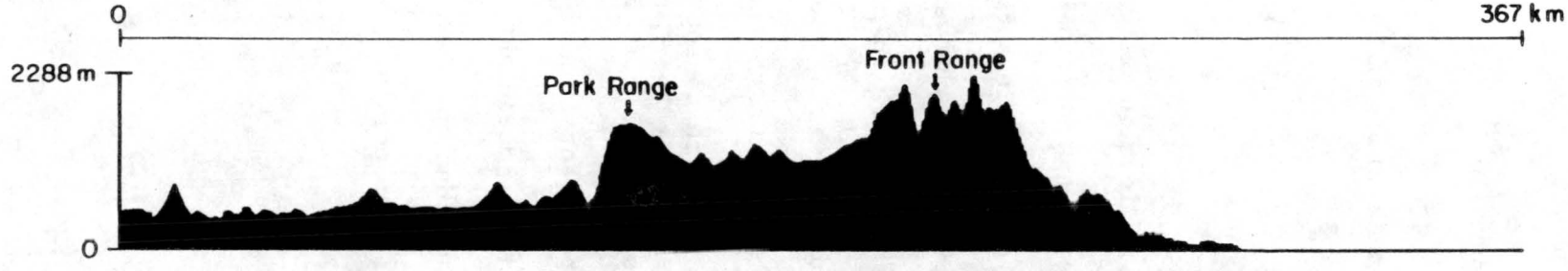

Figure 1. West to east cross section of the COSE topography with a thirty second longitude resolution taken at 40°30′ N latitude.

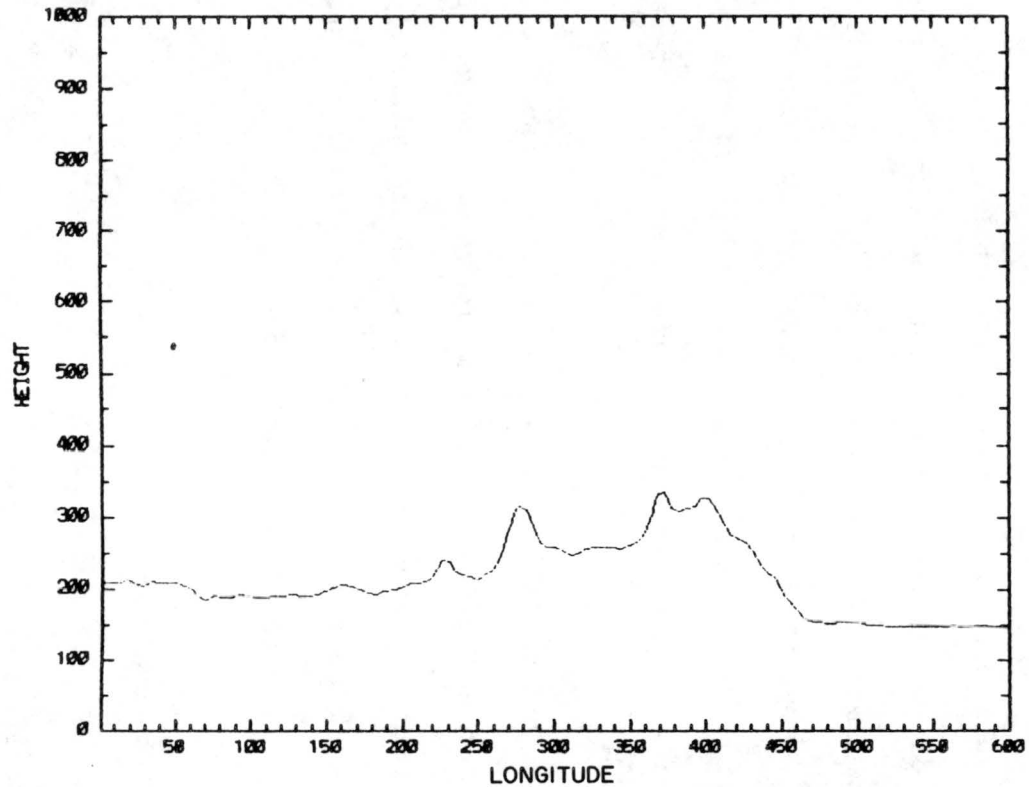

Figure 2. West to east cross section taken at 39° latitude averaged over 4° latitude. This smoothed version of the topography was used in model simulations.

Chapter 4. COSE FIELD OBSERVATIONS

The field data used to test the ability of RAMS to simulate orographic clouds was collected during the third Colorado Orographic Seeding Experiment (COSE) which took place from December 1981 to January 1982 near Steamboat Springs, Colorado in the Yampa Valley. The instrumentation used during this project has been thoroughly described by Uttal (1985) and Rauber (1985). A brief summary is presented in this chapter.

The purpose of COSE was to characterize orographic clouds over the northern Colorado Rockies and their microphysical characteristics. The Steamboat Springs area was chosen because of the relatively flat upwind fetch of the Park Range. Thus, the main orographic influence on clouds which form in this area is the Park Range.

4.1 Ground Observations

i. Dual-Channel Microwave Radiometer

This instrument, developed by the National Oceanic and Atmospheric Administration (NOAA) measures total liquid water and water vapor in a cloud system integrated along a column of air determined by the orientation of the antenna beam. The antenna rotates with respect to

elevation and azimuth angles. For storms during COSE, the antenna was set at a 15° elevation angle and was allowed to rotate 360° in the azimuthal plane. The radiometer measures microwave emission of liquid water at 31.65 GHz and water vapor at 20.6 GHz. Ice emission is not detected by these channels so liquid and vapor are isolated. In this study, the measurements of liquid water (in millimeters) is examined for the presence of liquid water and the changes it undergoes. The radiometer was placed at the base of the Steamboat Springs Ski Area 6 km west of the crest of the Park Range at 2050 m MSL (Hogg et al., 1983; Uttal, 1985; Rauber, 1985).

ii. Ku-Band Radar

The CSU Ku-band radar was designed for application to cold orographic clouds. A detailed description of the instrument is given in Rauber et al. (1982). This 1.79 cm wavelength vertically pointing radar detects ice particles. The measured reflectivity is a function of the sixth power of particle radius. Because supercooled water droplets are so small, the contribution to the reflectivity measurement is negligible. Measurements were made every 30 seconds with a vertical resolution of 100 m up to 8 km. These data were interpreted to give a history of cloud reflectivity and the vertical extent of the cloud. This instrument was collocated with the NOAA microwave radiometer. (Rauber, 1985; Uttal, 1985).

iii. Rotorod Measurements

Cloud liquid water content was measured at Storm Peak Laboratory at the crest of the Park Range using the Metronics, Inc. Rotorod described by Rogers et al. (1983) and Hindman et al. (1983). These measurements were used to imply the amount of liquid water present over the barrier in the lower parts of the cloud.

iv. Probe Stations

The Bureau of Reclamation supplied Portable Remote Observations of the Environment (PROBE) surface weather stations. These stations were scattered over the Yampa Valley upwind of and on the Park Range barrier. Data was continuously collected during COSE and the precipitation measurements have been used to some extent in this study.

v. Rawinsondes

During storm periods, the COSE team launched rawinsondes at 3 hr intervals from Craig, Colorado, approximately 60 km upwind of the barrier. These soundings were used to initialize the numerical model used in this research.

vi. Crystal Observations

Ground based crystal observations were made at six sites located from Craig, CO east to Storm Peak Laboratory (SPL) along the valley and up the barrier. These observations were made in 15 min intervals while snow was falling. Crystals were allowed to fall on framed black felt of 250 cm^2 in area and were classified according to the criteria established by Magono and Lee (1966). Ice particles were divided into single crystals and aggregates. The number of ice crystals per aggregate was counted and recorded. In addition, the amount of riming was identified as light, moderate or heavy. These data were used both to classify the microphysical characteristics of the storms examined and to study the evolution of the storms examined.

Precipitation intensity was measured at the radar/radiometer site (RAD) by collecting snow in a plastic bucket with a 160 cm^2 opening. The snowfall over a 15 min period was weighed and the precipitation intensity was calculated.

4.2 Synoptic Data

The synoptic evolution of these storms was examined using surface and upper air maps produced by the National Weather Service (NWS) as well as satellite photos provided by the Cheyenne, Wyoming office of the NWS.

4.3 Aircraft Data

The Colorado International Corporation (CIC) supplied their Cheyenne II aircraft. The flight paths taken by this aircraft are presented with the individual case studies in Chapter 5. The data used in this study included liquid water contents and ice crystal sizes and concentrations measured by the Particle Measuring Systems Forward Scattering Spectrometer Probe (FSSP) and the Two Dimensional Cloud Optical Array Probe (2D-c). Decelerator slides were analyzed with respect to the crystal characteristics observed at various points in the cloud. Ice crystals were allowed to impact on a slide coated with mineral oil. These slides were photographed under magnification (Uttal, 1985). This instrument is described in detail by Cooper and Vali (1981).

Chapter 5. CASE STUDIES

Portions of two storms studied during COSE were chosen for numerical simulation based on the dominant formation mechanism observed in the precipitation at the ground. From the first storm a period of heavy riming was used to test that portion of the model microphysics. Similarly, a heavy aggregation event during the second storm was simulated. A detailed description of these storms and the numerical simulations conducted is presented in this chapter.

Field data collected during each of these storms is presented in a manner to facilitate comparisons with model results. Model output is produced for the entire domain, but comparisons are limited to the specific areas studied in the field. The methods of data collection and the location of the collection sites were described in Chapter 4.

Numerical simulations were conducted as described in Chapter 3 and then compared against the field observations. Discrepancies found from these comparisons were used to develop the numerical experiments conducted for both cases and described in Chapter 6.

5.1 21 December 1981: Riming Case Study

The storm chosen to test the riming parameterization occurred on December 21, 1981. This storm has been classified as a post frontal case

and thoroughly described by Rauber (1985). The following section provides a reanalysis and reinterpretation of those data for easier comparisons with the RAMS predictions.

The surface frontal passage occurred at 0600 UTC. This front divided a very warm southern airmass and modified polar air to the north which was moist to 45 kPa. Rauber (1985) conducted a θ_e analysis to produce evidence that low level convection may have occurred below the stable frontal layer.

The storm can be broken into two distinct phases. Data collection began at 1200 UTC and the first phase of the storm continued until a distinct change in the precipitation characteristics was observed at 1400 UTC. The second phase, which extends from 1400 UTC, was chosen as a case study in which ice particle riming growth prevailed.

i. Stage I

During the first phase of the storm, precipitation intensity was classified as moderate to heavy. Aggregation was seen to decrease with time as riming increased from light to heavy. Planar and spatial dendrites dominated the crystal characteristics.

ii. Stage II

In the second phase, a distinct change in the precipitation characteristics occurred as aggregation almost disappeared at the crest and the base of the barrier. Rimed and unrimed needles were seen in addition to snow pellets. Nearly all particles were rimed. Precipitation

intensity remained moderate to heavy at the crest, but became light at the base of the barrier. Further upwind, light precipitation with heavy rime was observed. Crystal habits were obscured by the heavy rime. Light to heavily rimed aggregates were present during most of this phase.

Radar echo tops increased 1 km to between -24°C and -32°C or 5.8 and 6.5 km MSL (figure 3). Radar reflectivities remained near -10 to -5 dBZ. The highest values were seen in the middle parts of the cloud with local maxima from 0 to 5 dBz. Radiometer measurements slowly decreased by 0.2 mm to between 0.3 and 0.4 mm of liquid water. Ground level measurements at SPL have values of 0.1 to 0.15 g/m^3.

The research aircraft flight took place during this phase of the storm and was limited to regions in the cloud above 4 km MSL. Measurements of liquid water and ice water were taken from the leeside of the barrier out to 60 km west of the barrier. All of the liquid water observed was above 5.3 km MSL. The maximum values observed were over the barrier near cloud top in concentrations between 0.03 and 0.09 g/m^3 with droplet concentrations between 50 to 70 cm^{-3}. In the lower levels of over the barrier between 5.3 and 6.0 km MSL, liquid water contents averaged between 0.04 and 0.07 g/m^3 with droplet concentrations of 30 to 60 cm^{-3}. Upwind, near Craig between 5.5 and 6.0 km MSL, liquid water contents were lower and ranged from 0.03 to 0.05 g/m^3. Droplet concentrations were nearly the same (40 to 70 cm^{-3}). On the lee side of the barrier near cloud top between 6.2 and 6.7 km MSL lower liquid water contents of 0.02 to 0.05 g/m^3 were observed with lower droplet concentrations of 40 to 50 g/m^3.

Descriptions of the ice water measurements have been made by Rauber (1985) and Grant et al.(1982). Through analysis of the decelerator slides, Rauber found ice crystal characteristics were dominated by

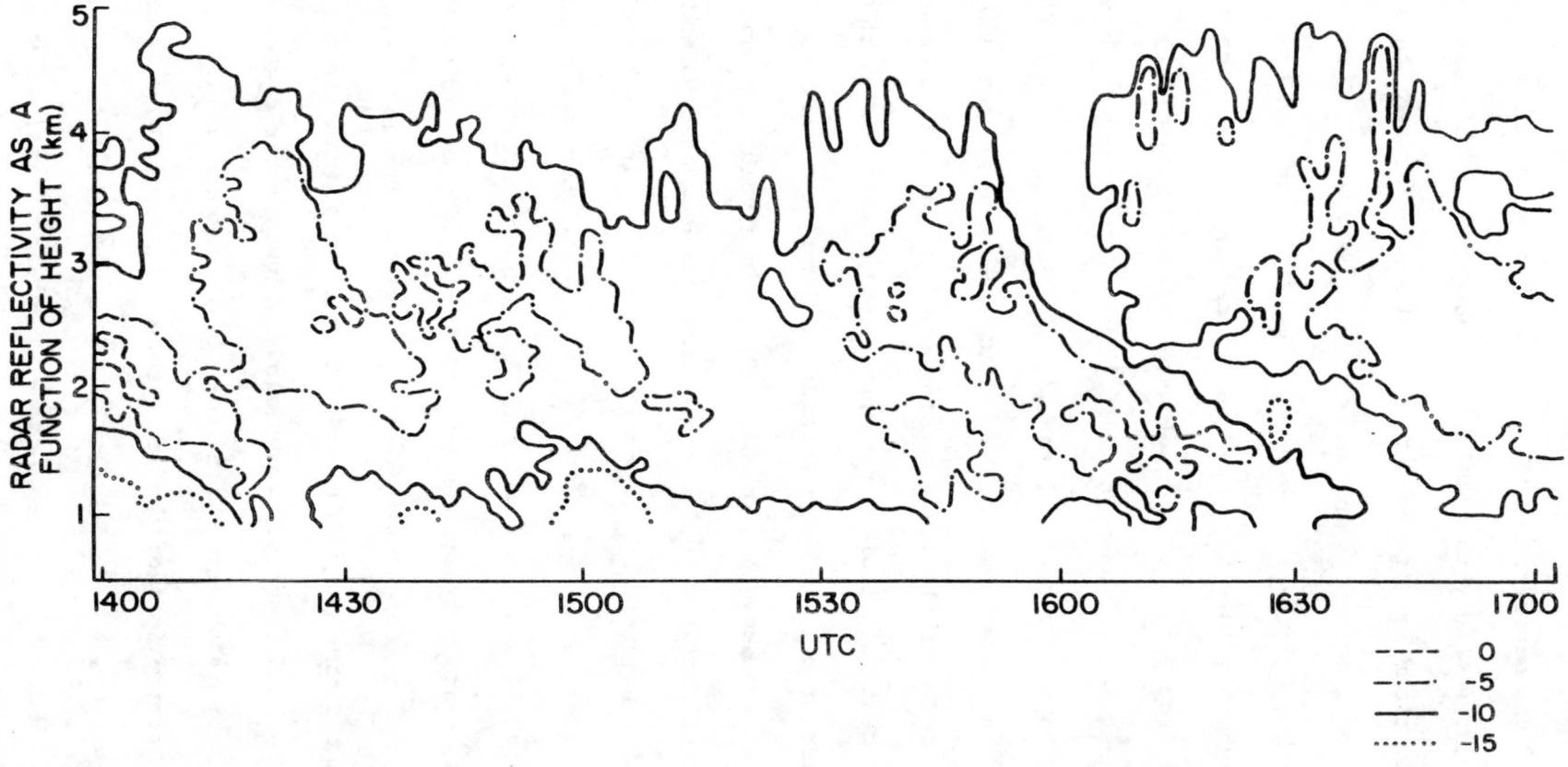

Figure 3. Radar reflectivity in dBZ as a function of height contoured for the time period from 1400 UTC to 1700 UTC on 21 December 1981.

hexagonal plates. Columns, bullets, long columns and cross-column assemblies were also noted. Upwind of the barrier in the upper levels of the cloud, frozen water droplets and rimed particles were observed giving some evidence that some rining was occurring in the upper levels of the cloud.

Grant et al. (1982) provided a detailed analysis of the ice crystal concentrations observed during this storm by the research aircraft. Crystal concentrations have been averaged in terms of the level in the cloud at which the measurements were made. A distinct increase in the average concentration was seen as the aircraft moved to lower levels of the cloud. In the upper levels of the cloud between -28.5 and -26.5°C, concentrations averaged 3.3 ℓ^{-1}. A slight increase was seen in the mid-levels where ice crystal concentrations average 5.9 ℓ^{-1}. A distinct increase of 3 to 6 times that seen in the higher levels was observed in the lowest levels of the cloud measured which were between -16.5 to -20.5°C. At these low levels, concentrations averaged 19.4 ℓ^{-1}.

Looking at the horizontal distribution of ice crystals in the upper levels, the 3 to 5 ℓ^{-1} concentrations seen over the barrier are only slightly higher than the 2 to 3 ℓ^{-1} seen on the leeside of the barrier. This suggests that only weak vertical motion could have been present at this level. In the lower parts of the cloud between -15 and -19°C, the concentrations both upwind and downwind of the barrier were approximately 10 ℓ^{-1}. Concentrations were observed to increase 3 to 4 times over the barrier to approximately 35 ℓ^{-1}. The sizes of the crystals at this lower level had a distribution with the mode near 100 to 200 μm.

5.2 5 January 1982: Aggregation Case Study

The second case study was taken from a storm which occurred on January 5, 1982 in which aggregation dominated the precipitation characteristics. Rauber (1985) classified this as a pre-frontal storm. A short wave trough moved quickly through the COSE area. Warm advection occurred throughout the troposphere until 1800 UTC. An upper level cold front moved through between 1800 UTC and 2100 UTC after which cold advection was seen above 600 mb. There was also a slight lowering of the moist layer.

This storm evolved in three stages. The third stage is used for the case study on aggregation because of the quasi-steady state the storm achieved and the resulting steady period of unrimed aggregation observed at the ground.

i. Stage I

During the first stage, between 1300 UTC and 1445 UTC, the area was enveloped by a shallow orographic system. Light precipitation fell in the form of heavily rimed crystals.

Late in the first stage, from 1400 UTC to 1445 UTC, a wide region of deep cloud moved toward the area. Precipitation became light and did not extend to Craig. No aggregates were observed. Echo tops decreased 1 to 2 km and reflectivities decreased 10 to 15 dBZ, and the radiometer detected substantial amounts of supercooled liquid water.

ii. Stage II

The second stage, from 1445 UTC to 1530 UTC, was a transitional period from when the deep cloud system from Utah entered the COSE area to when the storm achieved a quasi-steady state. Precipitation increased from moderate to heavy. Heavy rime was observed initially, but completely stopped by 1530 UTC. Aggregates of irregulars as well as planar and spatial dendrites dominated the precipitation characteristics seen at the ground crystal observation sites.

The physical characteristics of the cloud changed substantially from the previous stage. Cloud echo tops increased to near 8 km MSL yielding cloud top temperatures of approximately -36°C. At low levels radar reflectivities increased to values of 0 to 5 dBZ. The radiometric liquid water depth was reduced to zero.

During this portion of the storm, the research flight began, which allowed a more detailed analysis of the cloud structure. Liquid water contents were seen in concentrations from 0.07 to 0.10 g/m^3 over the barrier while upwind concentrations were less than 0.02 g/m^3. Cloud droplet concentrations were seen to increase to between 20 and 40 cm^{-3} throughout the cloud below 6.5 km MSL with the maximum concentrations of 70 cm^{-3} observed at 4.6 km MSL at the beginning of the transition in the second stage. The droplet size distribution showed modes from 0 to 4 μm which indicated new condensation (Blumenstein, 1982). In lower parts of the cloud near the barrier several points showed a second mode at 16 to 24 μm.

Ice crystal habits observed at -13°C during this transition period on the lee side of the Park Range, consisted of plates and cold

temperature columns but were mostly fragmented particles. Crystal concentrations were 40 to 80 l^{-1} at temperatures colder than -22°C . At mid levels of the flight path from -22°C to -17 °C, concentrations varied from 80 to 110 l^{-1} while at warmer temperatures concentrations were as high at 140 l^{-1}.

iii. Stage III

After 1530 UTC, the storm reached a steady state and a 2 hr period of aggregated precipitation began. Precipitation remained heavy. Riming stopped and aggregates of planar and spatial dendrites as well as irregulars dominated. This portion is classified as the third stage and was used for the aggregation case study.

Cloud echo tops lowered to 6.7 km MSL and -26°C. Radar reflectivities remained the same from the transition phase with local maxima still 5 to 10 dBZ. The liquid water depth measured by the microwave radiometer remained near zero. Liquid water contents in the lower parts of the cloud measured were 0.01 g/m^3. An ascent made by the aircraft over RAD and a descent over North Park on the lee side of the Park Range showed negligible water. Cloud droplet concentrations decreased to 10 cm^{-3} at lower levels between 4.2 and 4.6 km MSL with even less at higher levels. The size distribution was at 2 to 4 μm in diameter.

Ice crystals became columnar at -17°C. Concentrations reduced to between 20 and 40 l^{-1} at temperatures colder than -17°C and 40 to 80 l^{-1} between -17 and -13°C. The size spectra at the beginning of this stage showed the majority of the particles were less than 400 μm in diameter.

5.3 21 December 1981: Numerical Simulation

The riming case study has been simulated previously and described in Cotton et al. (1985) and Mulvihill et al. (1986). As described in Chapter 3, each of the model simulations was initialized using a sounding taken at Craig, CO.

Figure 4 is the temperature, moisture and wind sounding used to initiate the model simulation. The wind profile plotted is the westerly component of the measured winds. Near 400 mb the sounding was moist enough for this layer to be filled with cloud as it was lifted orographically. The temperature profile showed a conditionally unstable layer between 760 mb and 610 mb with a well defined frontal inversion from 610 mb to 580 mb. Above this level the atmosphere was stable. The 700 to 500 mb winds backed with height indicating cold advection and a frontal passage. Also, a 78 m/s jet maximum occurred at 300 mb while winds at 500 mb were much lighter at 24 m/s.

After the airflow was allowed 3 hr to achieve a steady state, the microphysics in the model was activated and allowed to run for an additional 2 hr. The simulated fields after this 5 hr simulation were analyzed and compared against what was observed in the field.

Model predictions are contoured over the smoothed COSE topography. The portion of the domain appearing in these plots is marked on the COSE topography in figure 5. The value of z is equal to 1.4 km less than the MSL height. The dark line shown in each of the figures is the outline of the cloud boundary predicted by the model. This line is equivalent to a 1/100 g/kg contour line of liquid water.

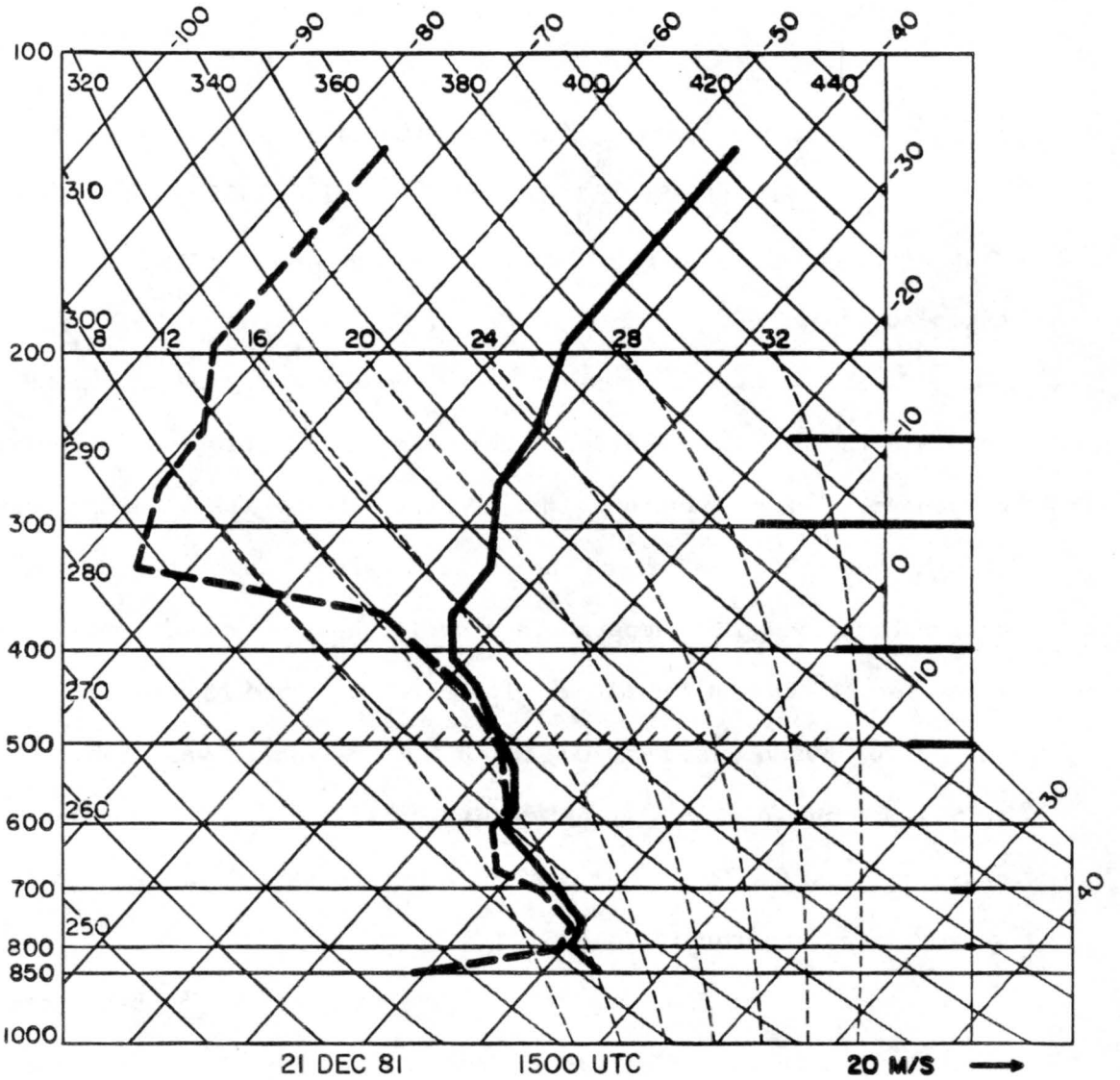

Figure 4. Sounding at 1500 UTC on 21 December 1981 taken at Craig, CO. Temperature curve is represented by the solid line, dew point temperature by the dashed line. The westerly component of the wind is plotted along the far right side.

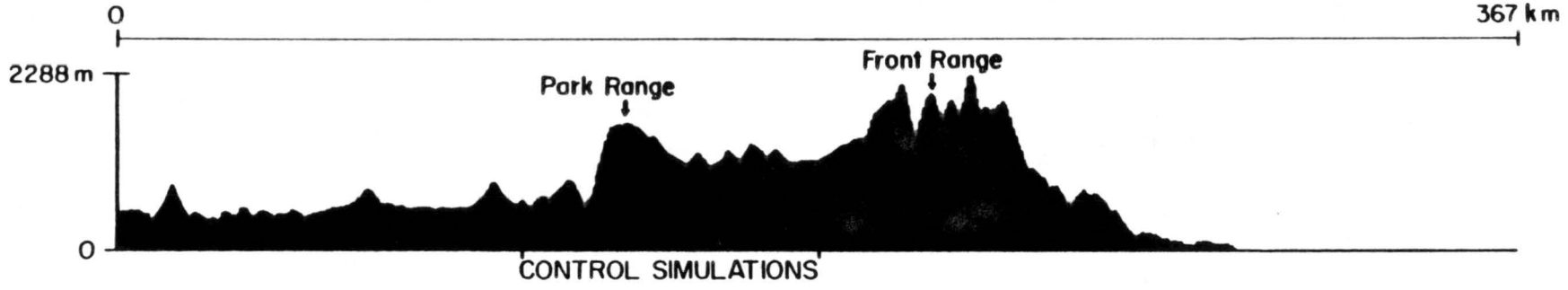

Figure 5. COSE topography marked with area depicted in control simulation results.

i. Cloud Water

Figure 6 shows the mixing ratio of cloud water in g/kg contoured over the smoothed topography. The cloud boundary, which appears in all of these figures, shows tops which are more variable than those determined by the vertically pointing radar in Figure 3. Tops are predicted at 6.1 km MSL while the radar reported echo tops between 6.0 and 6.5 km MSL. It is possible that the convective elements suggested by the radar reflectivities may be mirrored by the model produced cloud outlines.

Looking more closely at this figure, the cloud water distribution can be examined. Most of the cloud water was predicted below the aircraft flight path. Ground level rotorod measurements taken at SPL gave values of 0.1 to 0.15 g/m^3. The model predicted highest values near the barrier to be 0.05 g/kg. Values observed by aircraft were 0.03 to 0.09 g/m^3 near cloud top over the barrier. This compares to less than 0.01 g/kg predicted. Over the barrier between 5.3 and 6.0 km MSL, the observed liquid water content was 0.04 to 0.07 g/m^3 this compares with predicted values up to 0.02 g/kg. To the lee side of the barrier between 6.2 and 6.7 km MSL, values of 0.02 to 0.05 g/m^3 were observed while no liquid water was predicted here. To the west, near Craig, between 5.5 and 6.0 km MSL liquid water contents were between 0.03 and 0.05 g/m^3. Here again, no liquid water was predicted at this height. Droplet concentrations observed by the aircraft were between 30 and 60 cm^{-3}. A constant value, equal to the number of cloud condensation nuclei, of 60 cm^{-3} was specified in the model. The amount of cloud water predicted by the model was consistently less than that observed. Discrepancies varied from one half to one tenth the observed values.

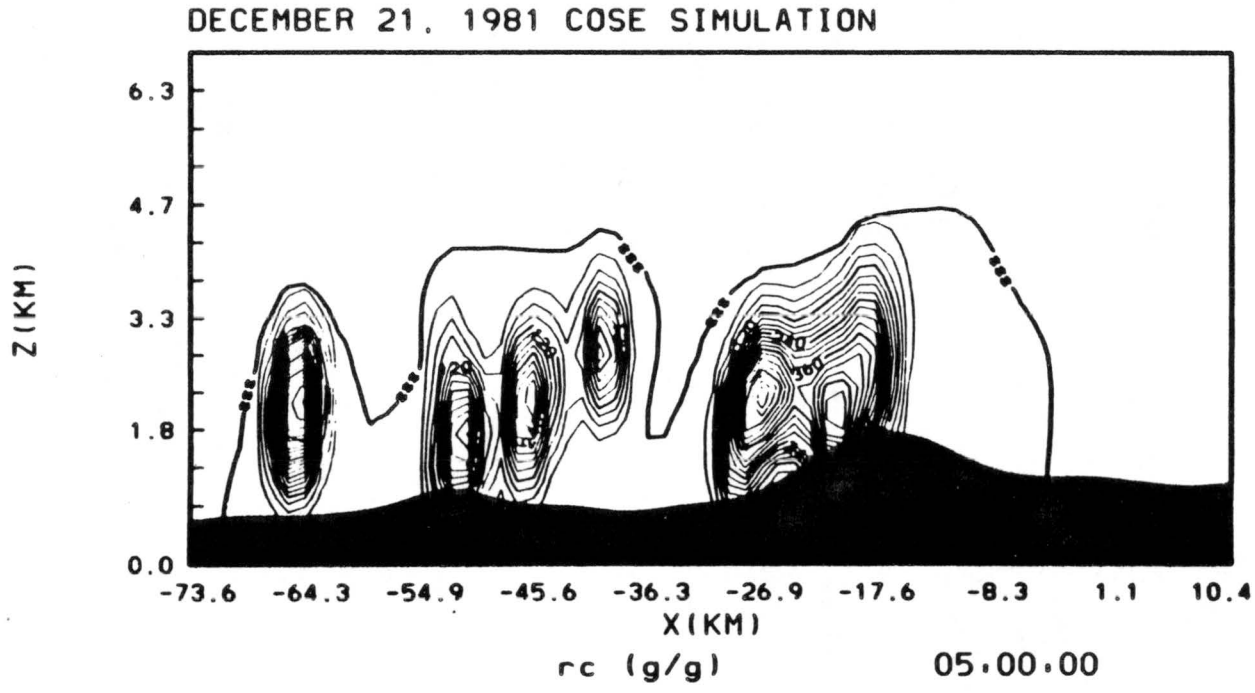

Figure 6. Mixing ratio of cloud water contoured over the smoothed COSE topography in intervals of 0.003 g/kg for the 21 December 1981 control simulation.

The predicted cloud boundary shows the variability in the cloud top. Thus, the possibility arises that the cloud did not reach the steady state necessary for comparisons between model predictions and the field observations. A more uniform orographic cloud may be better for these types of comparisons.

ii. Ice Crystal Concentrations

The ice crystal concentrations can be compared in a similar way. Figure 7 shows the logarithm of the predicted crystal concentrations plotted. Comparing this with data from the research aircraft, the RAMS predicted crystal concentrations well in that values were within an order of magnitude of observed values. At the highest levels of the cloud, the model correctly predicted concentrations of 1 to 3 l^{-1} compared to an average of 3.3 l^{-1} observed. At mid levels of the cloud between 5.3 and 5.8 km MSL, the model predicted concentrations of 0.3 to 1.0 l^{-1} which were on the same order of magnitude of observed values which averaged 5.9 l^{-1}. Similar concentrations were predicted for lower levels between 4.3 and 5.3 km, but 19.4 l^{-1} was the average observed concentration. Aircraft observations show a decrease in crystal concentrations with height, but RAMS predicted an increase in ice crystal concentrations with height. The RAMS prediction was described in Chapter 3. Cotton et al. (1986) suggested that the upper portions of the cloud are "clean". Little mixing of the boundary layer air with the upper levels in stable orographic clouds could account for the low level ice crystal concentration maxima observed.

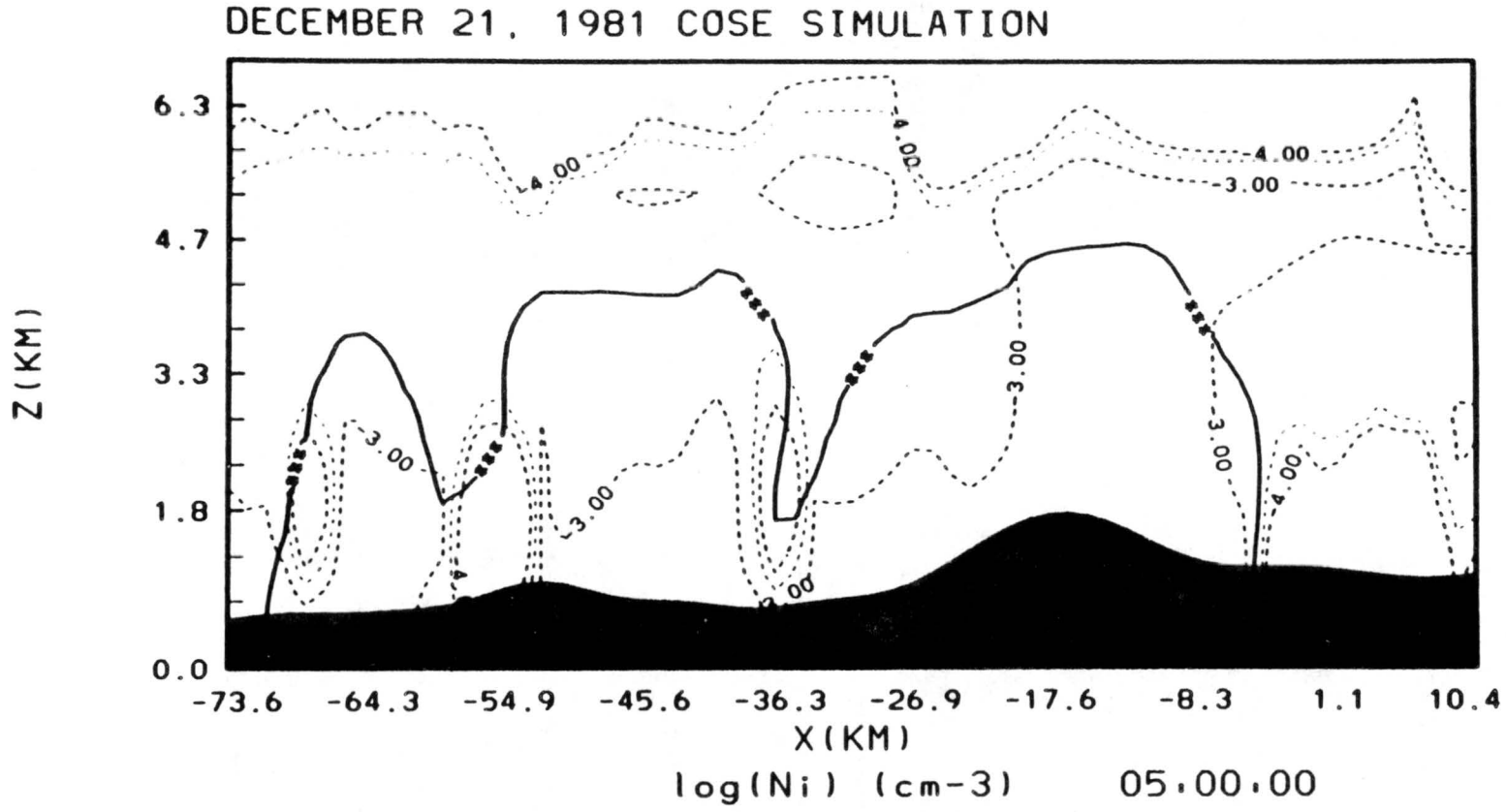

Figure 7. Logarithm of ice crystal concentration contoured over the smoothed COSE topography in intervals of 0.5 for the 21 December 1981 control simulation.

iii. Graupel

No graupel were predicted by the model in this simulation so it has been eliminated from the discussion. In Chapter 6 this problem is addressed.

iv. Aggregates

The last predicted quantity analyzed was the mixing ratio of aggregates plotted in figure 8. This was used to compare the spatial distribution of aggregates over the COSE area. As mentioned in Chapter 4, crystal observations were taken over six ground sites marked in figure 2. During this case study, aggregates were observed at all locations except RAD at the base of the barrier. Figure 8 shows that aggregates were predicted in other areas of the COSE domain, but not over RAD. The spatial distribution of the aggregates was predicted correctly. This distribution was affected by the dip in the cloud boundary above RAD. The cloud water figure also shows that other predicted quantities were lower in the area of RAD.

The mixing ratio of aggregates was further analyzed by calculating the percentage of hydrometeors predicted in the form of aggregates. Figure 9 shows this distribution which will be used to compare with the sensitivity tests in Chapter 6.

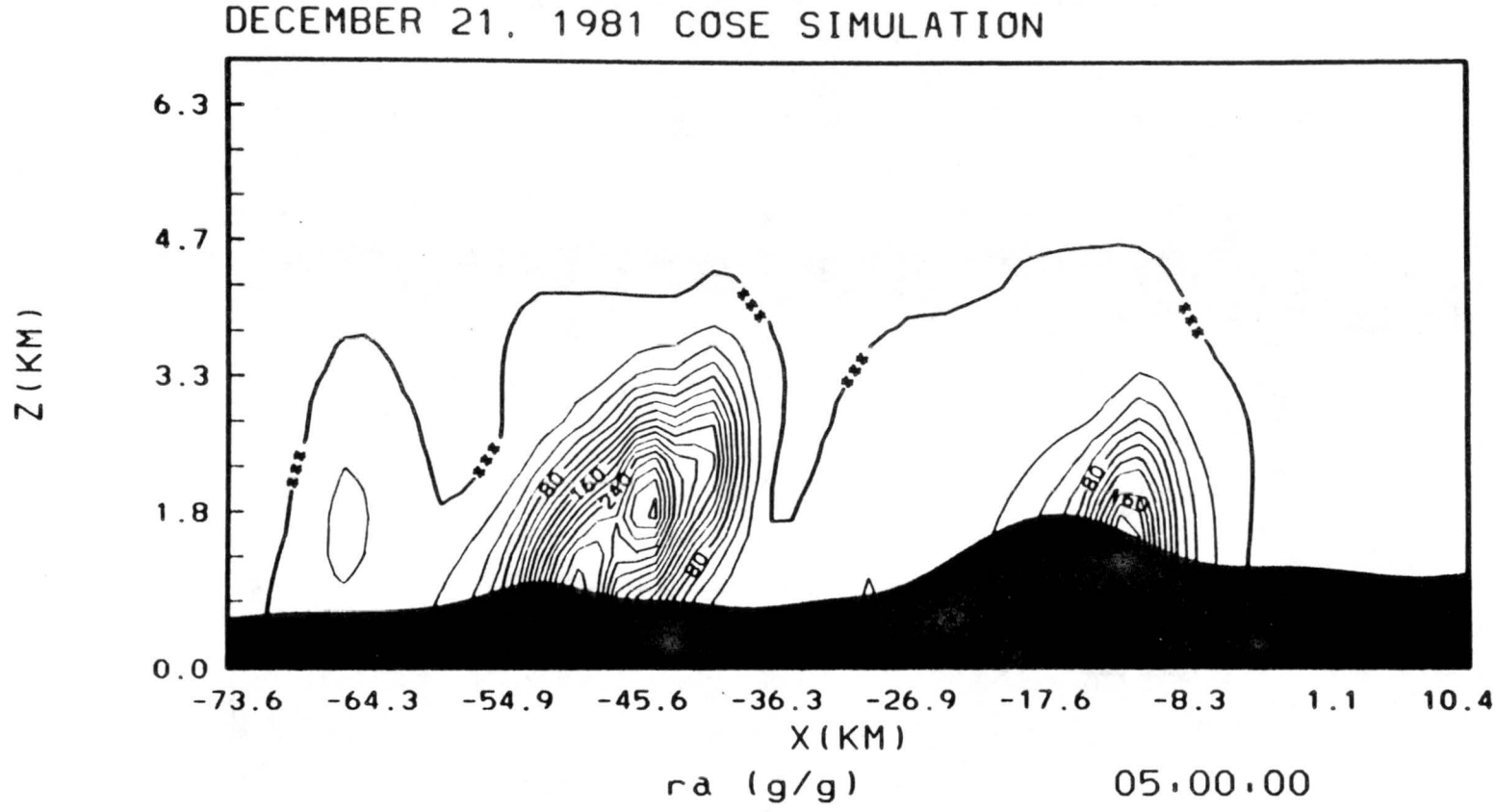

Figure 8. Mixing ratio of aggregates contoured over the smoothed COSE topography in intervals of 0.02 g/kg for the 21 December 1981 control simulation.

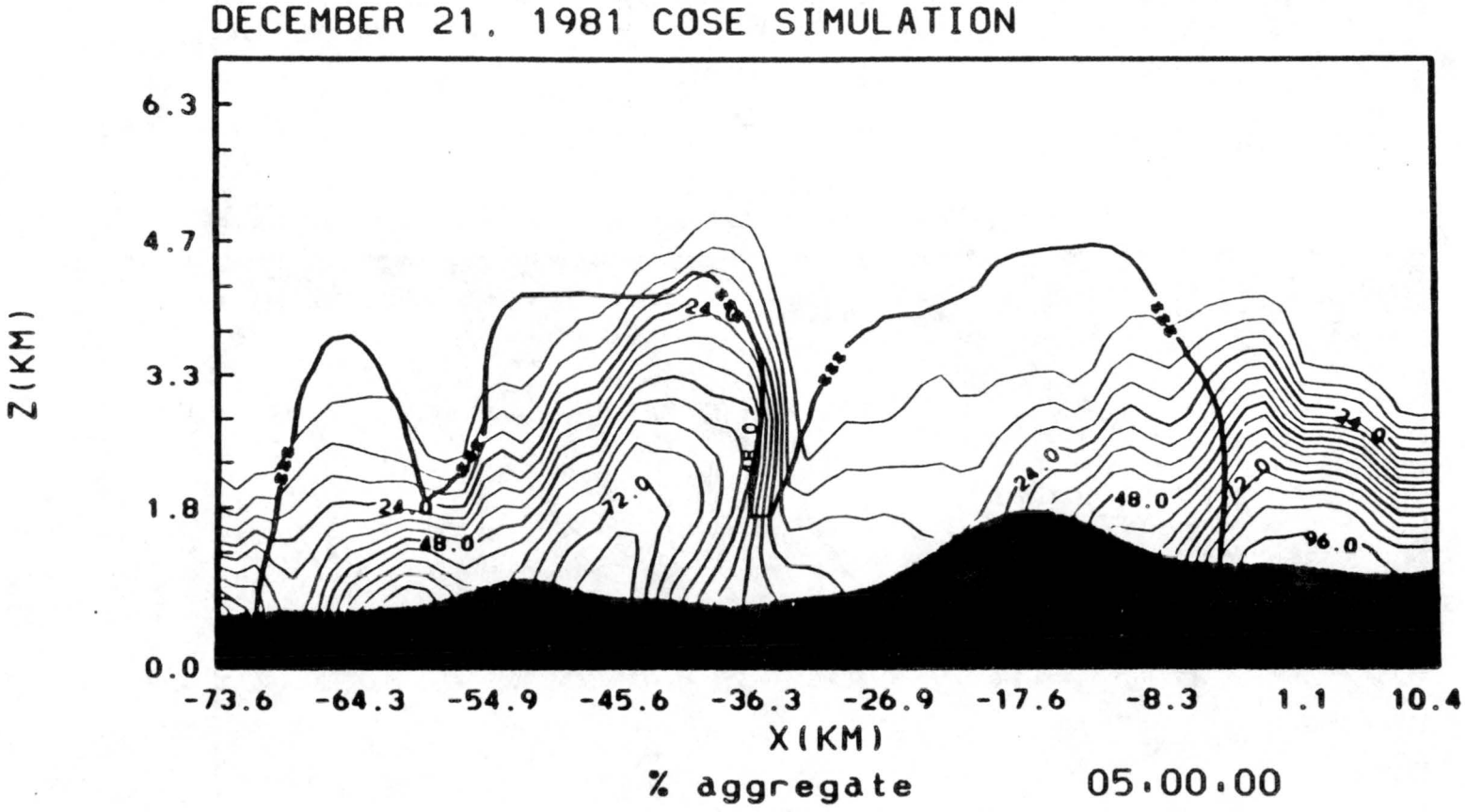

Figure 9. Percentage of precipitation predicted to be aggregates contoured over the smoothed COSE topography in intervals of 6 % for the 21 December 1981 control simulation.

5.4 5 January 1982: Numerical Simulation

The aggregation case study was initialized with the 1500 UTC sounding taken at Craig, CO on 5 January 1982. Previous simulations of this case have been described in Cotton et al. (1986) and Mulvihill et al. (1986).

Figure 10 is the sounding used. This sounding was used to initialize the temperature, humidity and wind profiles in the model. There are several important features. The sounding was saturated throughout much of its vertical extent. Also, the atmosphere was stable except for two conditionally stable layers between 760 mb and 690 mb and between 620 mb and 590 mb. The wind near 500 mb was relatively strong at 34 m/s, and the 700 mb to 500 mb winds veered implying warm advection.

The results of the RAMS simulations are plotted in figures 11 through 14. Each shows the cloud boundary was somewhat uniform at 9.2 km MSL with a slight dip to 8 km MSL above the lee side of the barrier.

i. Cloud Water

Cloud water, depicted in figure 11, was underpredicted compared to what was observed by the aircraft. Most of the cloud water was predicted in the lower parts of the cloud below the flight path making comparisons difficult. Amounts were predicted up to 4.7 km in values less than 0.01 g/kg. Negligible amounts of liquid water were seen in an ascent over RAD. Amounts were observed to be less than 0.01 g/m^3 along the flight path.

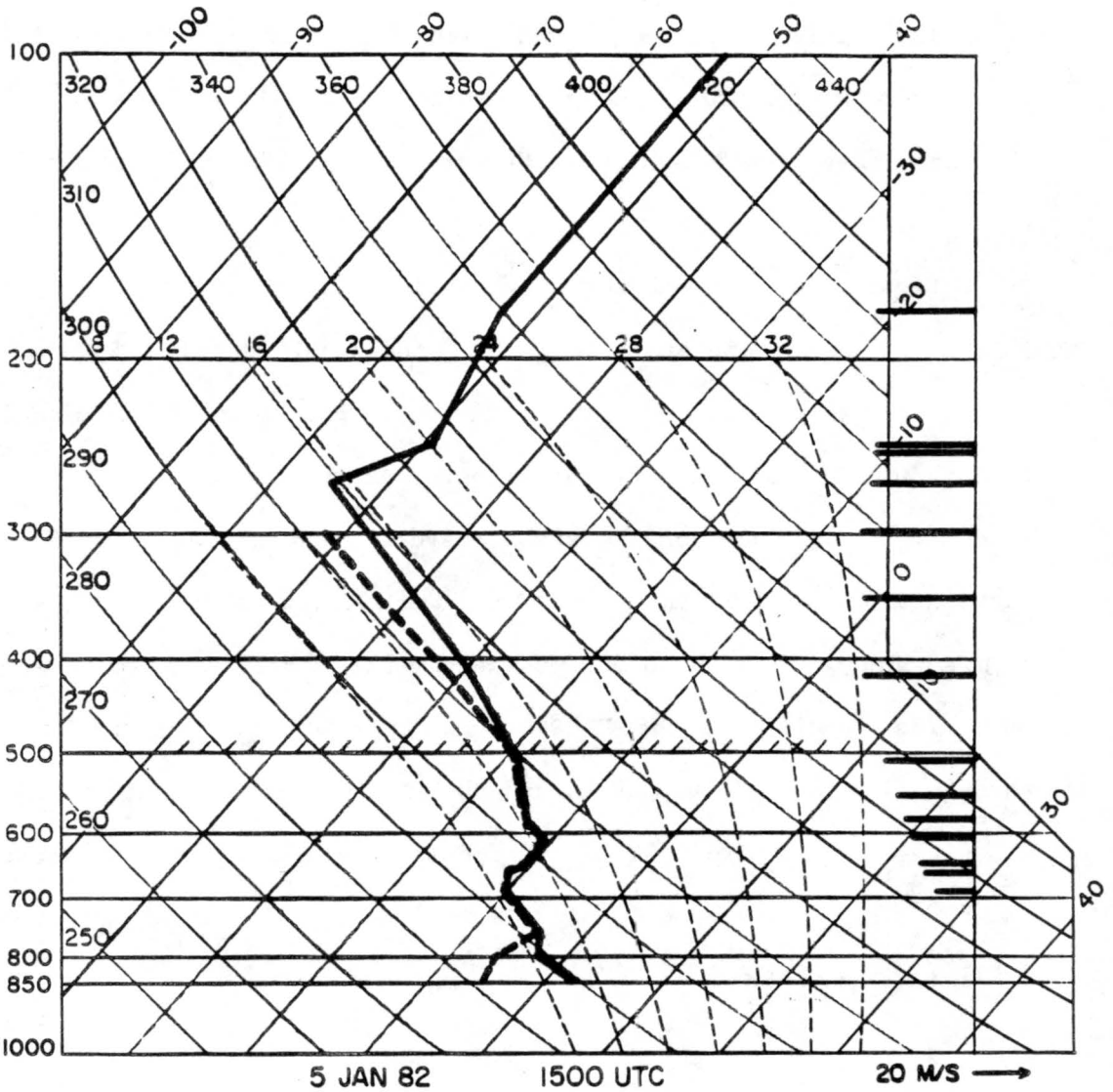

Figure 10. Sounding at 1500 UTC on 5 January 1982 taken at Craig, CO. Temperature curve is represented by the solid line, dew point temperature by the dashed line. The westerly component of the wind is plotted along the far right side.

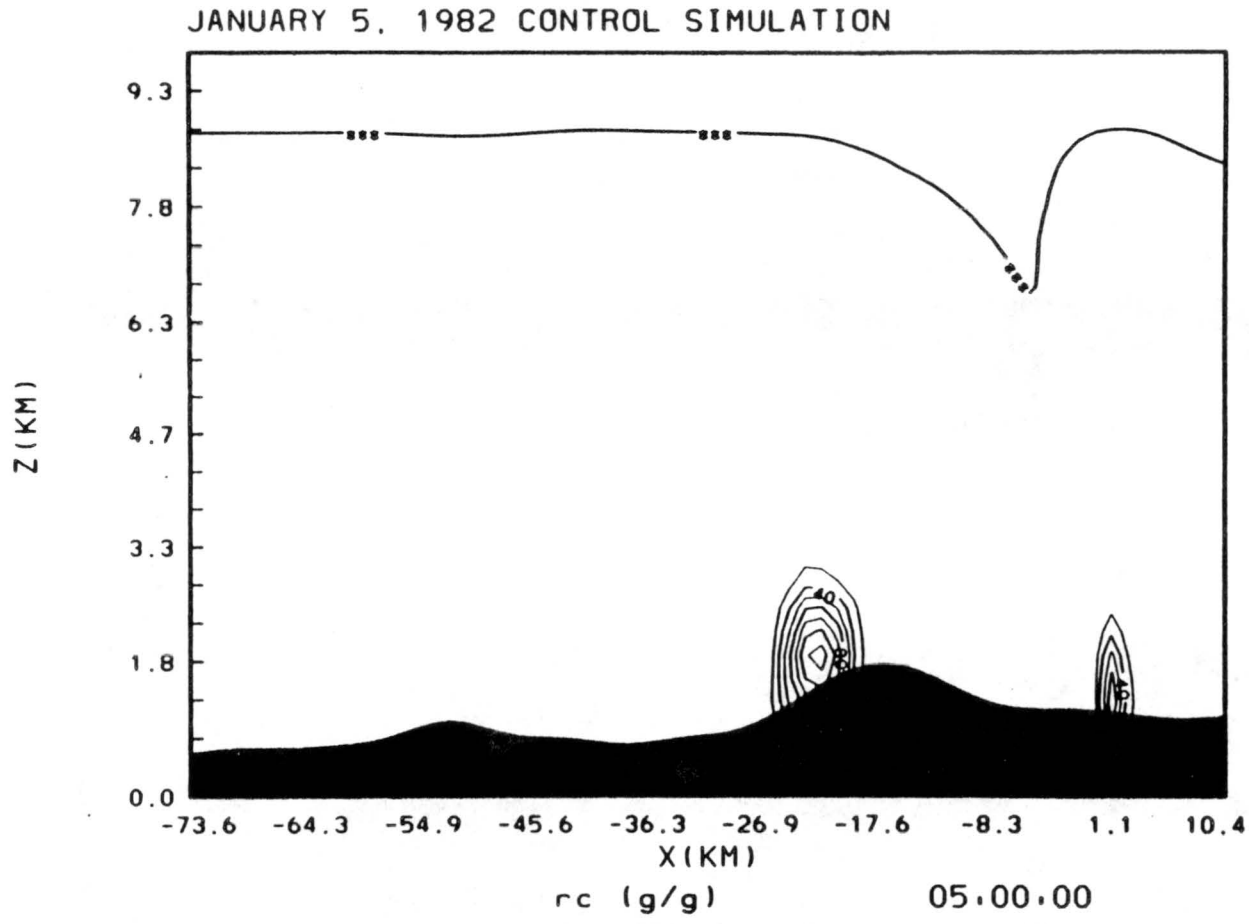

Figure 11. Mixing ratio of cloud water contoured over the smoothed COSE topography in intervals of 0.002 g/kg for the 5 January 1982 control simulation.

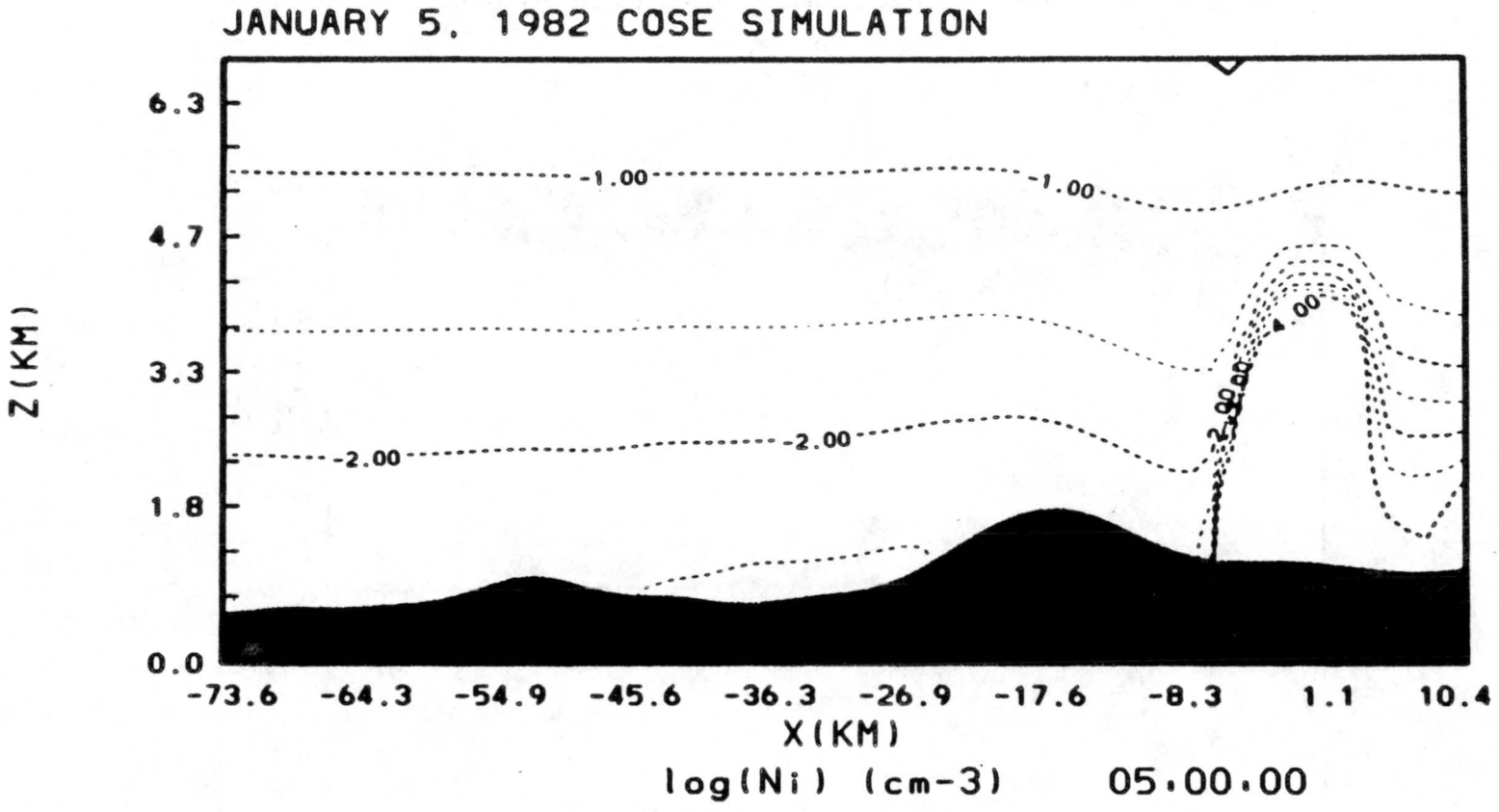

Figure 12. Logarithm of ice crystal concentration contoured over the smoothed COSE topography in intervals of 0.5 for the 5 January 1982 control simulation.

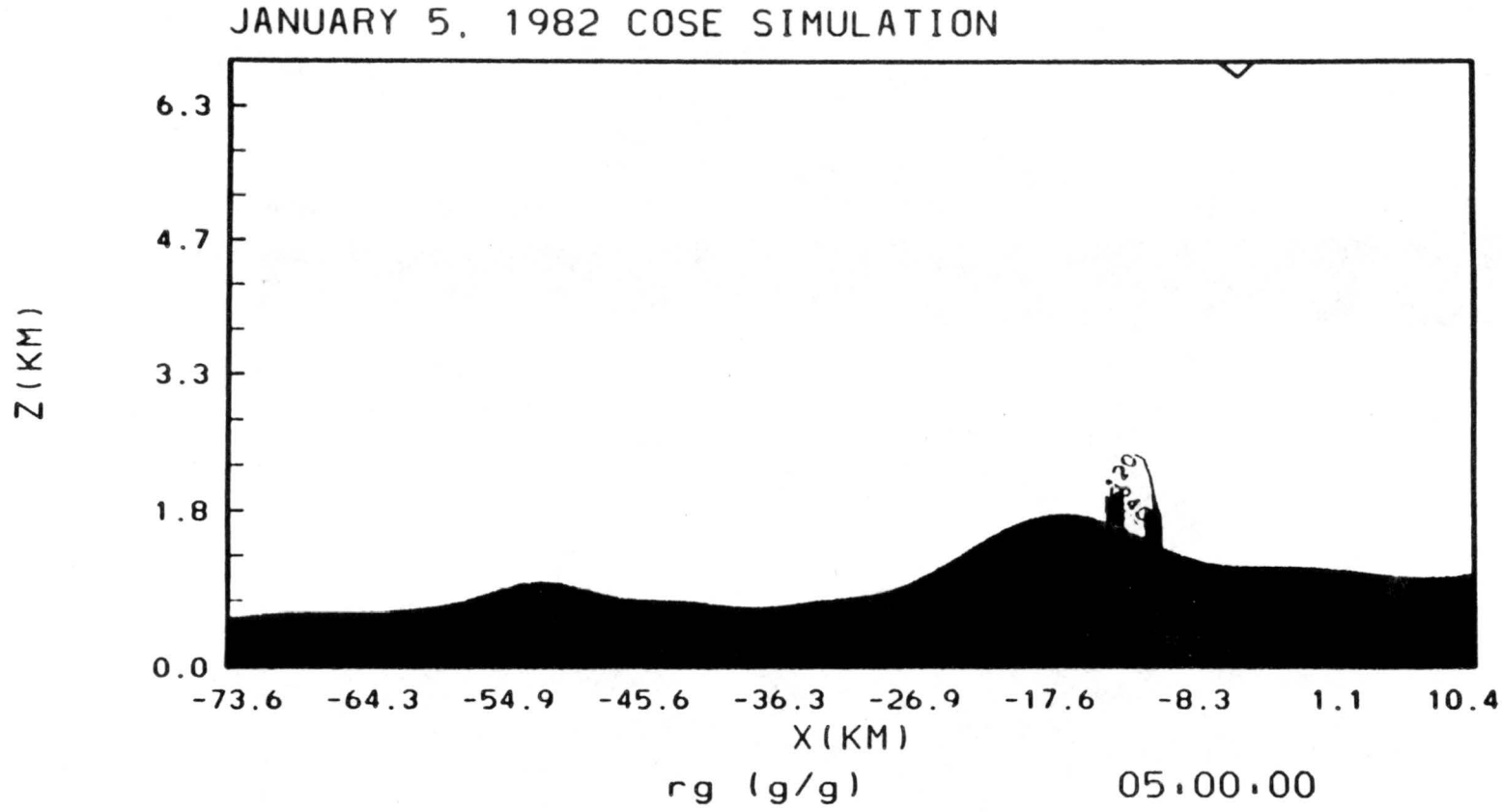

Figure 13. Mixing ratio of graupel contoured over the smoothed COSE topography in intervals of 0.02 g/kg for the 5 January 1982 control simulation.

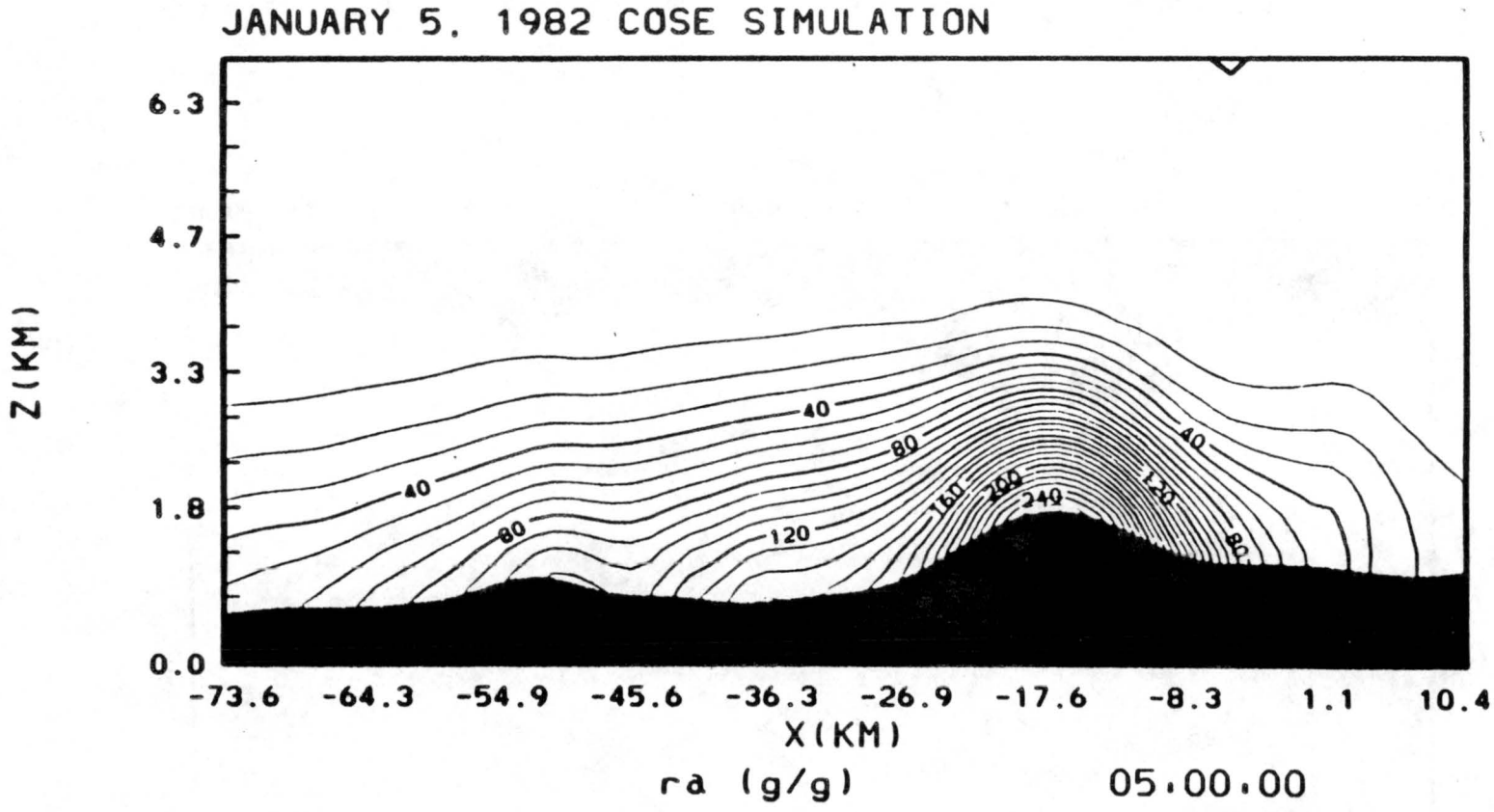

Figure 14. Mixing ratio of aggregates contoured over the smoothed COSE topography in intervals of 0.02 g/kg for the 5 January 1982 control simulation.

ii. Ice Crystal Concentrations

The concentration of ice crystals predicted is shown in figure 12. The predicted concentrations were within a factor of two of the observed values. The same problem found in the riming case study appears in this one. The observed concentrations decreased with height while the predicted concentrations increased with height. More specifically, at temperatures colder than -17°C the model predicted from 25 to over 100 l^{-1} compared to the 20 to 40 l^{-1} measured by the aircraft. Lower in the cloud between -13 and -17°C, the model predicted 25 to 10 l^{-1} compared to the 40 to 80 l^{-1} observed.

iii. Graupel

Graupel was predicted in an area where no observations were made as seen in figure 13. Therefore, comparisons with field data could not be made. The graupel was predicted downwind of the cloud water predicted above the western slope of the barrier as would be expected.

iv. Aggregates

Figure 14 shows the mixing ratio of aggregates predicted. Aggregates were observed at all the ground crystal observation sites. The model predicted aggregates over the whole domain.

The percentage of the precipitation which was predicted as aggregates has been plotted in figure 15 to further analyze the predictions. Calculations were made from observations at RAD to compare

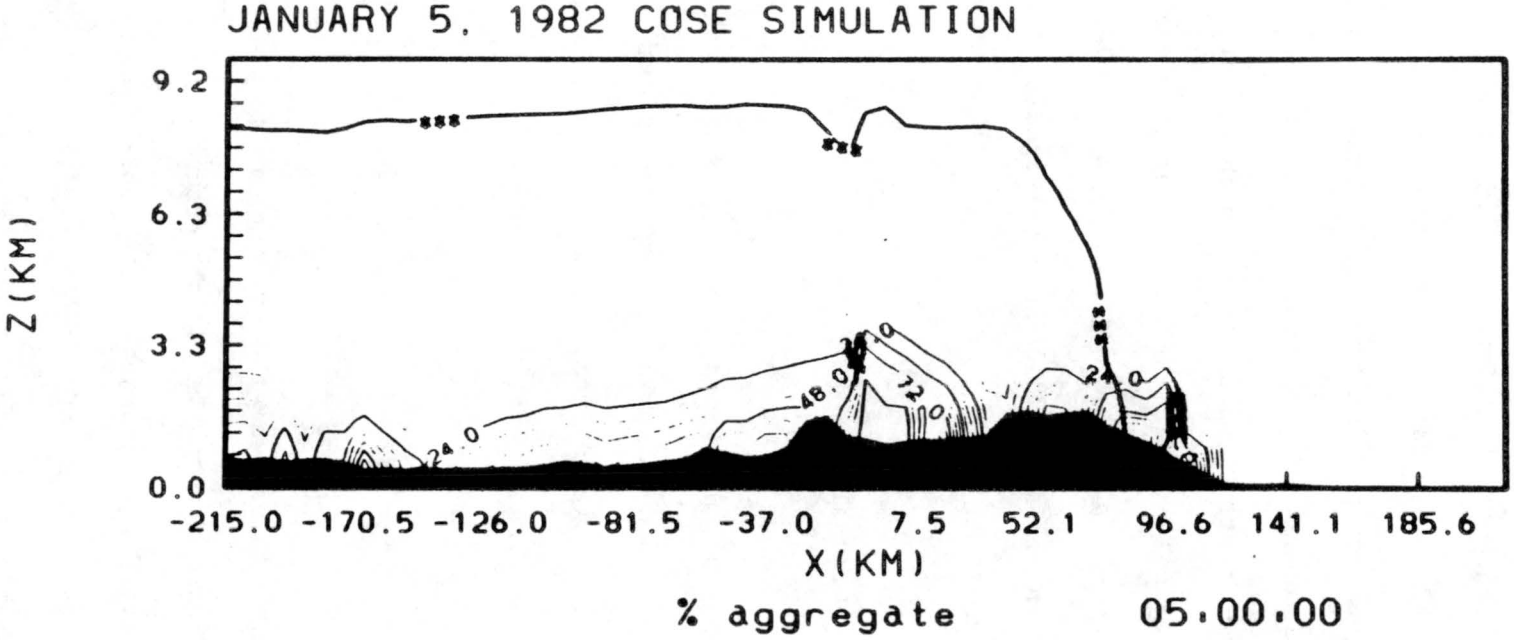

Figure 15. Percentage of precipitation predicted to be aggregates contoured over the smoothed COSE topography in intervals of 6 % for the 5 January 1982 control simulation.

to the model predictions. At SPL, virtually all crystals were seen in aggregates and at RAD, 95% of the crystals were in aggregates. The model predicted 60% of the precipitation was aggregates over RAD and 54% over SPL. The amount of precipitation predicted as aggregates was underestimated.

5.5 Summary of Comparison Studies

In this section comparisons are made between the two control simulations. Common discrepancies were used to develop the experiments discussed in Chapter 6.

The predicted cloud boundary compared well in the riming case but was several kilometers below observed echo tops in the aggregation case. A common problem arose in the cloud water mixing ratio predictions. The flight path of the research aircraft was above where the majority of the liquid water was predicted. This limited comparisons. In the regions where comparisons could be made, the model predicted lower values than were observed.

The concentration of ice crystals was predicted well. The best correlations between observed and predicted concentrations were seen in the upper levels of the cloud. In the lower levels of the cloud, concentrations were underpredicted. Also, a problem arose in the vertical distribution of the ice crystal concentrations. While the observed values decreased with height, the predicted values increased with height.

Graupel was not predicted in the riming case study and predicted in areas where observations were not made in the aggregation case. These results show that the prediction of graupel does not represent the prediction of the riming process.

The spatial distribution of aggregates observed was mirrored by the control simulations. In the aggregation case study, a calculation was made from the observed data to compare the percentage of the precipitation predicted as aggregates. This showed that the mixing ratio of aggregates contributed the greatest to the overall precipitation type, but did not dominate the precipitation characteristics to the same extent as was observed.

These discrepancies were used to develop the experiments discussed in the next chapter.

Chapter 6. SENSITIVITY TESTS AND EXPERIMENTS

6.1 Graupel Experiments

The equations for the conversion of ice to graupel and the conversion of aggregates to graupel have a threshold value which must be met before the conversion can take place. These threshold values may have inhibited the production of graupel in the cases simulated. For this experiment, the thresholds have been removed.

The equation for the conversion of ice to graupel is given by

$$CN_{ig} = \left[\max\left[CL_{ci} - \left(\frac{N_i}{\rho_o} \right) C_m, 0 \right] + CL_{ri} \right] h(T_c) \qquad (25)$$

where C_m is the characteristic diameter of a cloud droplet. The term which is subtracted from CL_{ci} is the threshold value. This equation was changed to remove the threshold. CL_{ri} is the collection of rain by ice and was removed because it is negligible in these cold clouds. Equation (25) simplifies to

$$CN_{ig} = \max\left[CL_{ci}, 0 \right] \qquad (26)$$

The conversion of aggregates to graupel is given by the equation

$$CN_{ag} = \max\left[CL_{ca} - \left[\frac{g\rho_o}{C_{D_r} D_{m_r}}\right]^{1/2} \left[\frac{1}{\rho_w^2 \rho_g}\right]^{1/4} \bar{r}_c \bar{r}_a, 0 \right] \tag{27}$$

$$+ \frac{0.25\left(R_m^2 + 1.7\, R_m D_{m_a} + 1.87\, D_{m_a}^2\right)}{\rho_w R_m^3} \rho_o \bar{v}_a - \bar{v}_r \bar{r}_a \bar{r}_r + CL_{ra}\, h(T_c)$$

where R_m is the characteristic diameter of a raindrop, v_r is the terminal velocity of a raindrop and r_r is the mean mixing ratio of rain water and CL_{ra} is the collection of aggregates by rain. The threshold value is the term subtracted from CL_{ca}. This was eliminated from the equation as well as the elaborate term added at the far right of the equation since negligible amounts of rain are predicted for these two cases. Equation (27) thus becomes

$$CN_{ag} = \max[CL_{ca}, 0] \tag{28}$$

i. 21 December 1981: Graupel Experiment

The purpose of this experiment was to force the prediction of graupel in the riming case study. The control simulation of this case showed that no graupel was predicted although ground based crystal observations showed heavy rime at all the sites. Figure 17 shows that graupel was predicted in bundles isolated under the blobs in the cloud boundary. Again, the mixing ratio seems to be dependent on the placement of the cloud boundary.

The cloud boundary changed from the control simulation (see figure 18). Crystal concentrations changed at lower levels. A decrease was

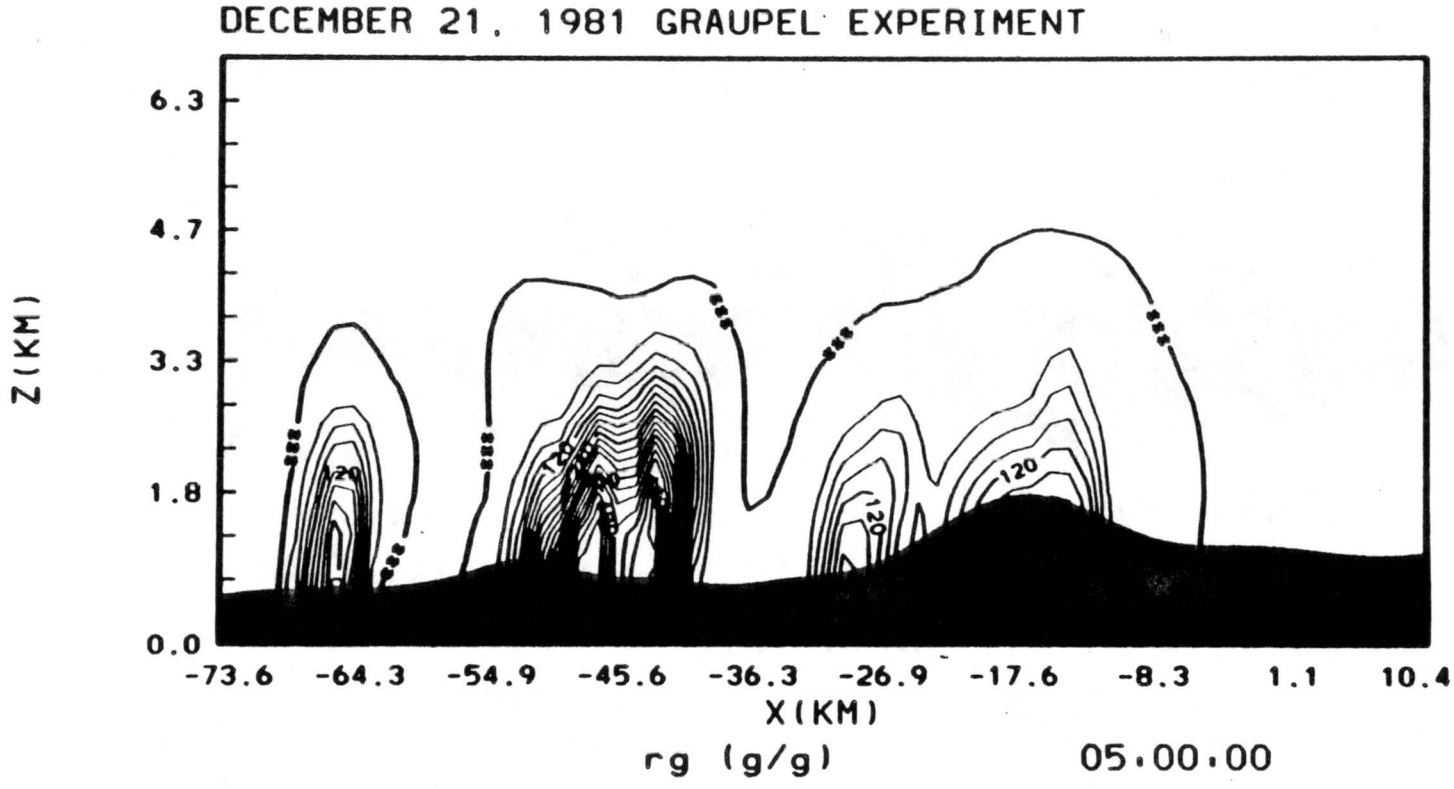

Figure 16. Mixing ratio of graupel contoured over the smoothed COSE topography in intervals of 0.003 g/kg for the 21 December 1981 Graupel Experiment.

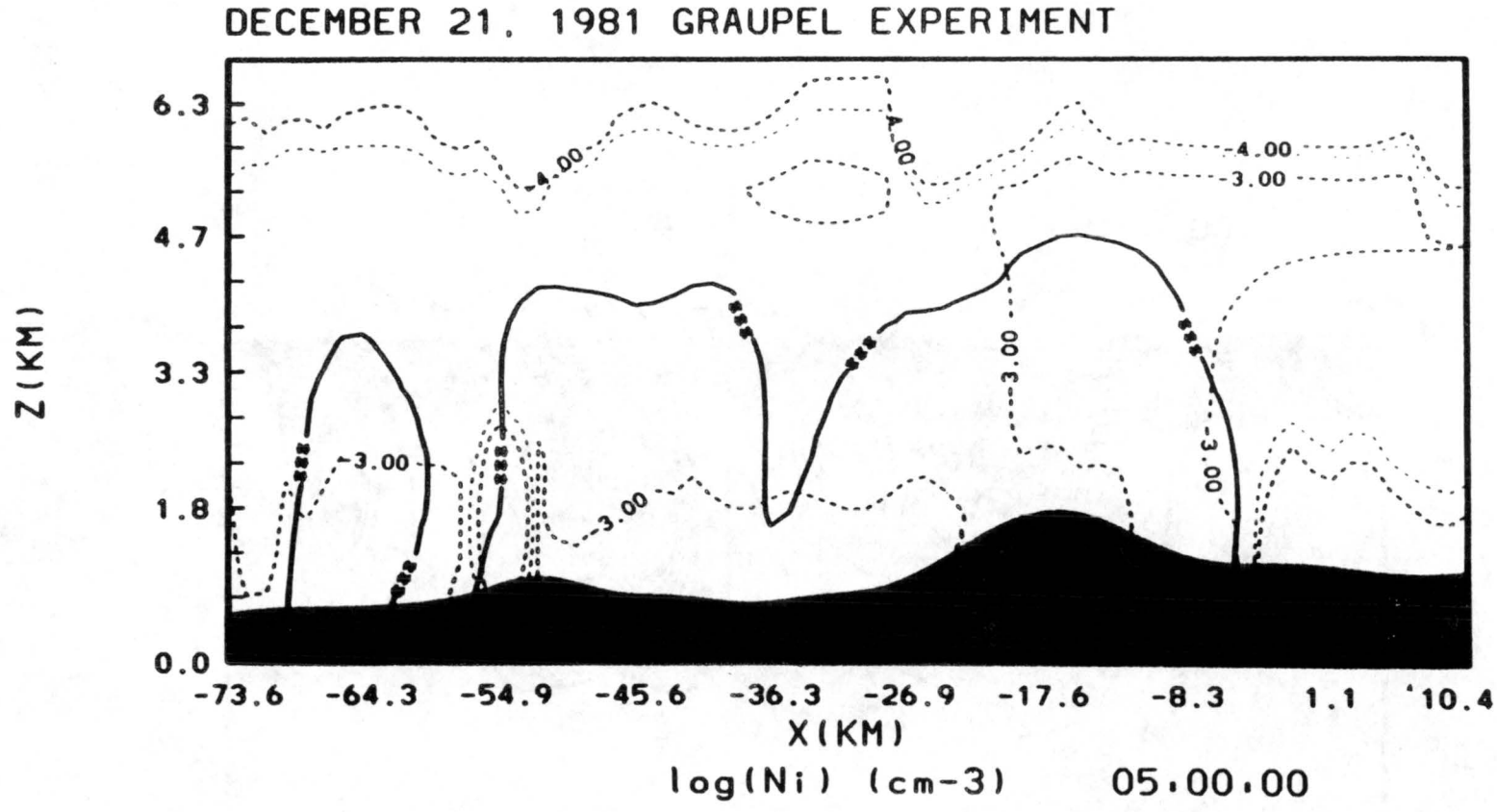

Figure 17. Logarithm of ice crystal concentration contoured over the smoothed COSE topography in intervals of 0.5 for the 21 December 1981 Graupel Experiment.

predicted over the crest and an increase was seen in the dip in the cloud boundary just west of the barrier. Ice mixing ratios were reduced to half of the control predictions. The differences were almost negligible, but the model had underpredicted the crystal concentrations in the control simulation. A reduction in the predicted values only caused a further discrepancy with the observed values.

Cloud water was predicted in similar amounts over the barrier, but more than doubled in value over the control experiment upwind of the barrier (see figure 18). Observations were made above the levels at which cloud water was predicted to the west of the barrier. Cloud water was still not predicted in the area observed.

The predicted mixing ratio of aggregates (figure 19) decreased to one half of the control values. The percent aggregates decreased in a similar way (figure 20).

ii. 5 January 1982: Graupel Experiment

In the control experiment, graupel was predicted over the eastern slope of the barrier. The main purpose of this experiment was to determine how the riming case study was affected, but it was also run on the aggregation case.

Figure 21 shows a broader distribution of graupel over the barrier. Mixing ratios almost doubled to a maximum value of 0.078 g/kg. The graupel predicted was seen to shift to the west with respect to the position predicted by the control experiment. The mixing ratios were similar between the two simulations. In this experiment the graupel has been predicted where the major area of cloud water was predicted in the

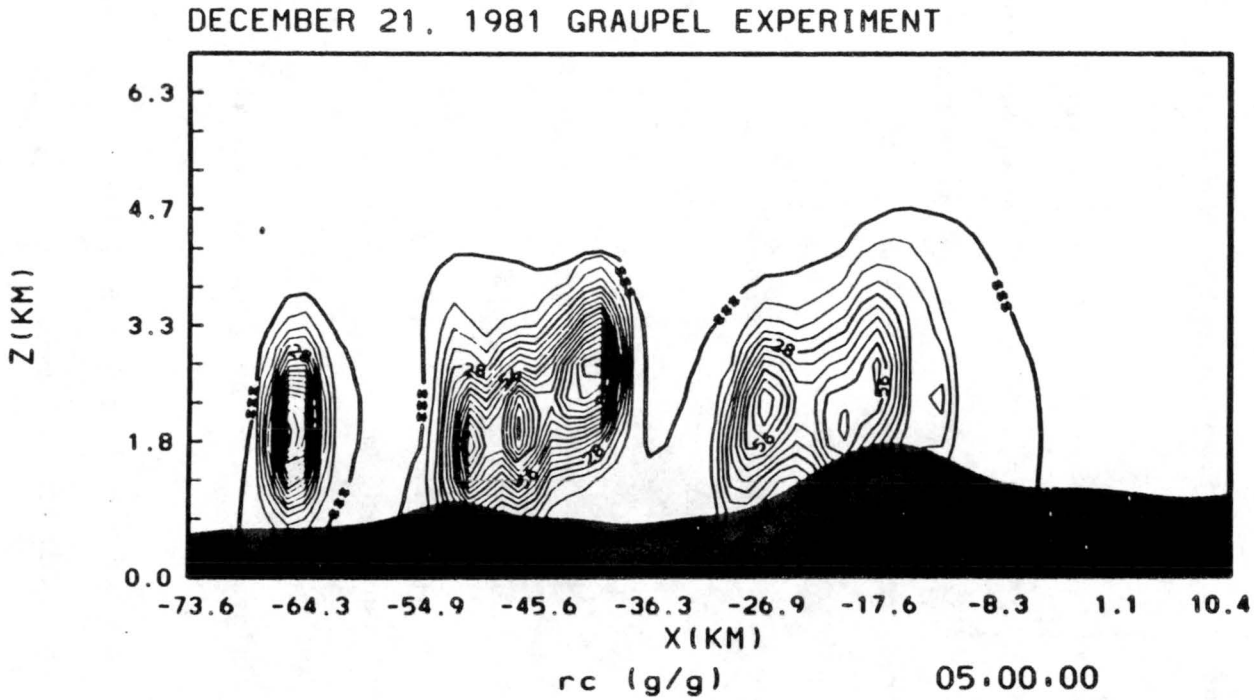

Figure 18. Mixing ratio of cloud water contoured over the smoothed COSE topography in intervals of 0.007 g/kg for the 21 December 1981 Graupel Experiment.

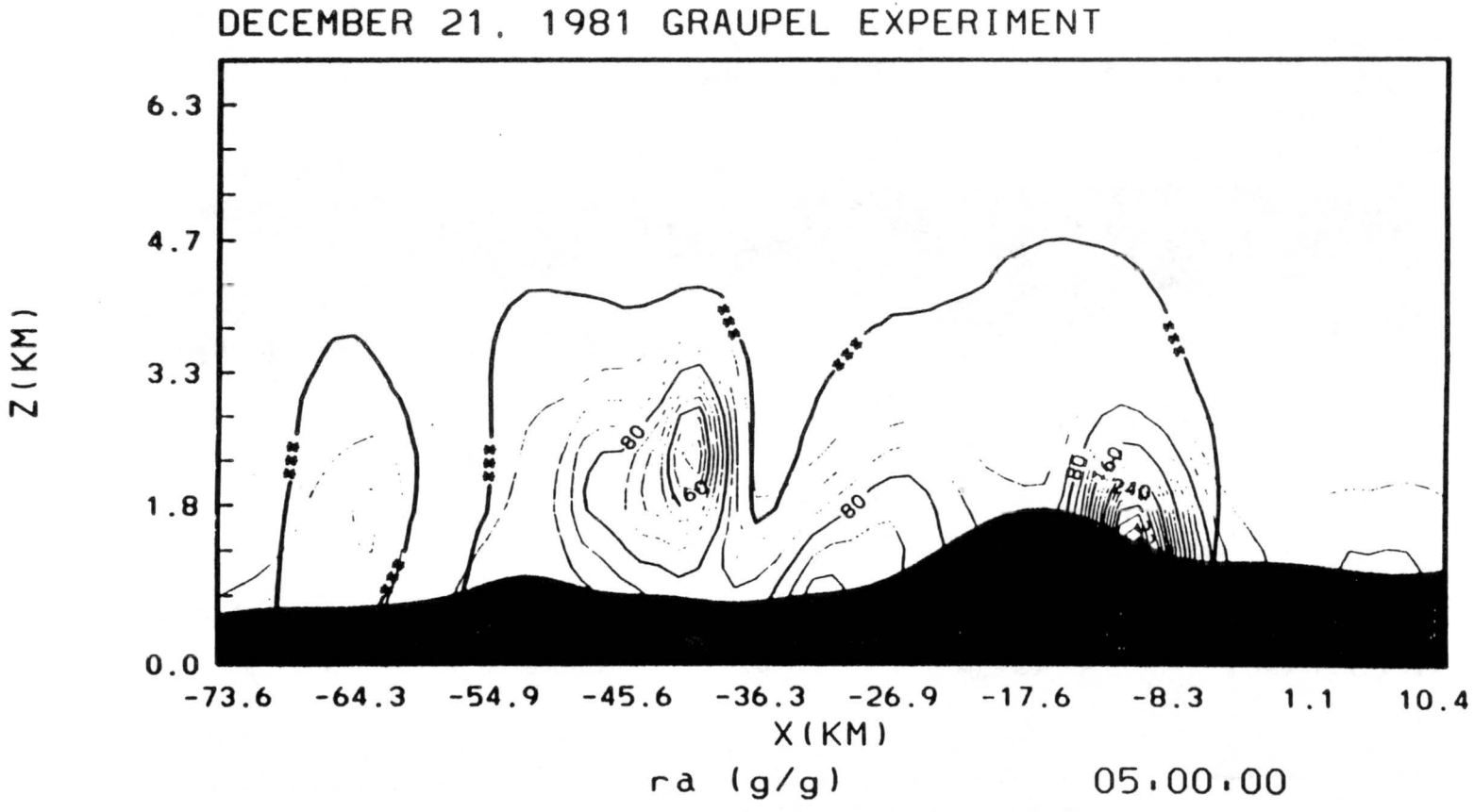

Figure 19. Mixing ratio of aggregates contoured over the smoothed COSE topography in intervals of 0.002 g/kg for the 21 December 1981 Graupel Experiment.

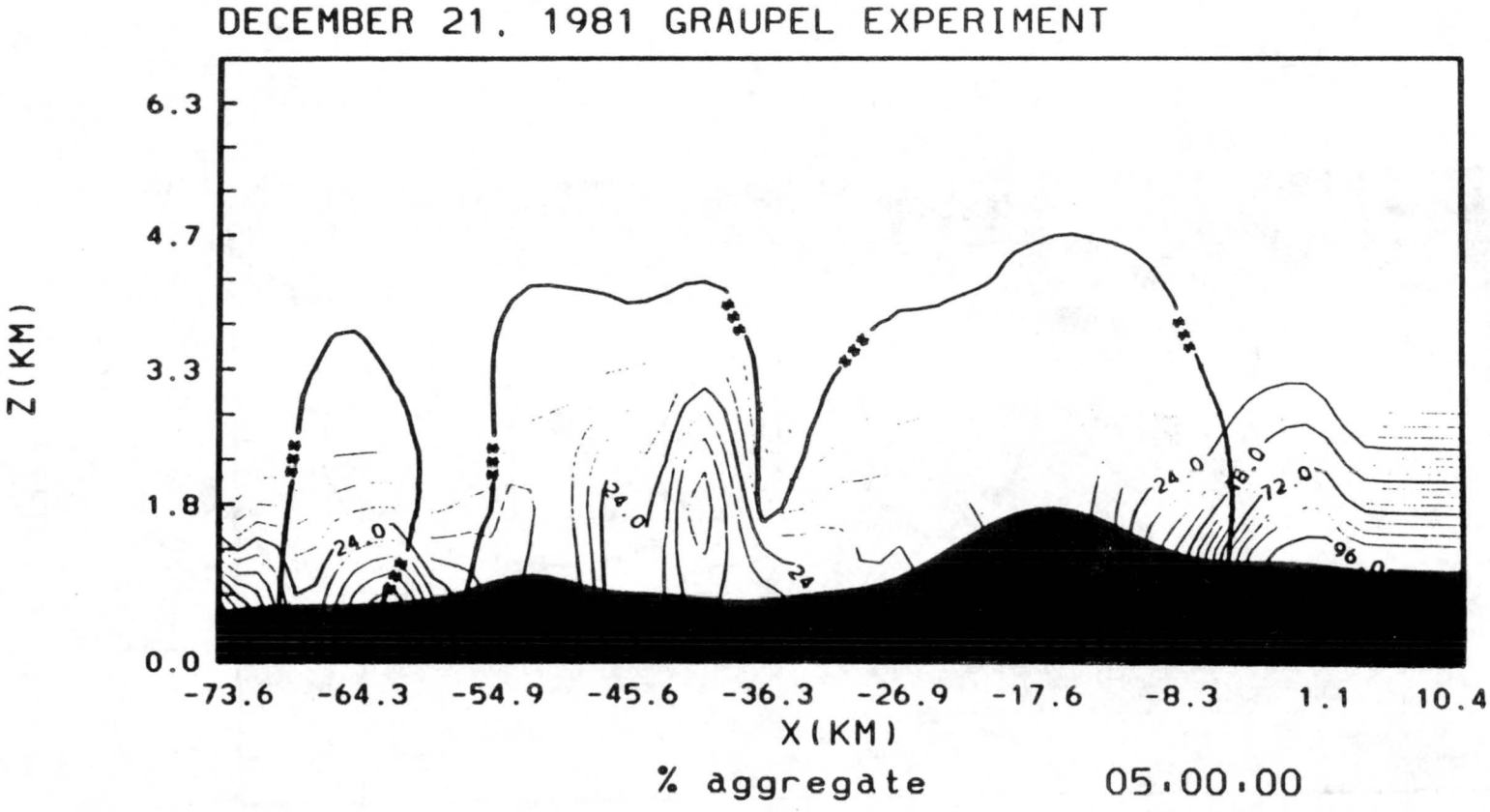

Figure 20. Percentage of precipitation predicted to be aggregates contoured over the smoothed COSE topography in intervals of 6 % for the 21 December 1981 Graupel Experiment.

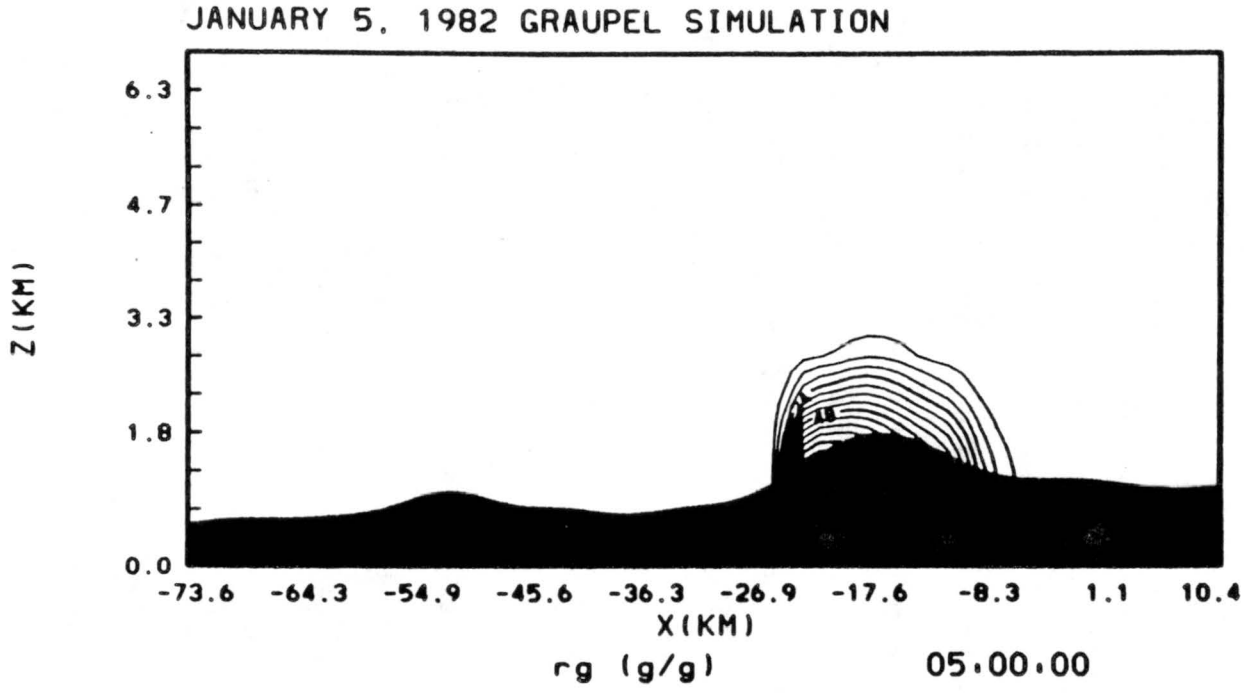

Figure 21. Mixing ratio of graupel contoured over the smoothed COSE topography in intervals of 0.006 g/kg for the 5 January 1982 Graupel Experiment.

control simulation. The lack of graupel on the lee side of the barrier may account for the increase in liquid water seen in that area.

Cloud water mixing ratio remained the same as the control over the barrier, but increased on the lee side (figure 22) at least doubling the value. The distribution was nearly identical to the control simulation and thus no closer to the observed values which were measured at higher levels in the cloud.

The mixing ratio of aggregates was reduced over the barrier where the graupel was predicted. The largest change in the aggregate mixing ratio was predicted at the crest of the barrier where there was a decrease of almost two thirds. The percentage of aggregates also shows a similar decrease in this region (Figures 23 and 24). This caused yet a greater underprediction of the percentage of aggregates than in the control.

6.2 Graupel Density Changes

The graupel experiment is taken one step further by using the modified conversion equations and by changing the graupel density. The density of graupel specified in the model was 0.6 g/cm^3. This value was chosen for the convective summertime clouds originally modeled by RAMS. Graupel tends to be less dense in wintertime orographic clouds. Prupacher and Klett (1979) summarized the results of the research performed in this area. For orographic snowfall, Locatelli and Hobbs (1974) found values of 0.05 to 0.45 g/cm^3 in the Cascade Mountains of Washington. Magono (1953) and Nakaya and Terada (1935) observed values of 0.13 g/cm^3 in Japan. Closer to Colorado, in Wyoming, Zikmunda and Vali (1972) found

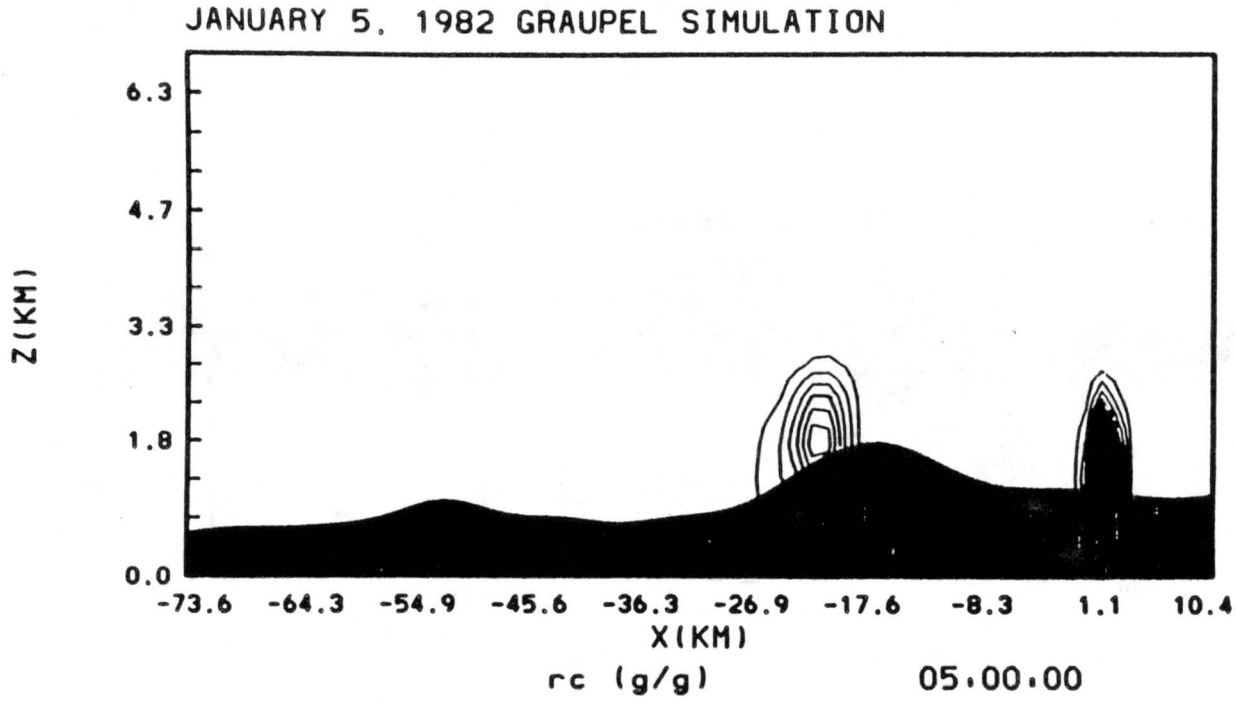

Figure 22. Mixing ratio of cloud water contoured over the smoothed COSE topography in intervals of 0.002 g/kg for the 5 January 1982 Graupel Experiment.

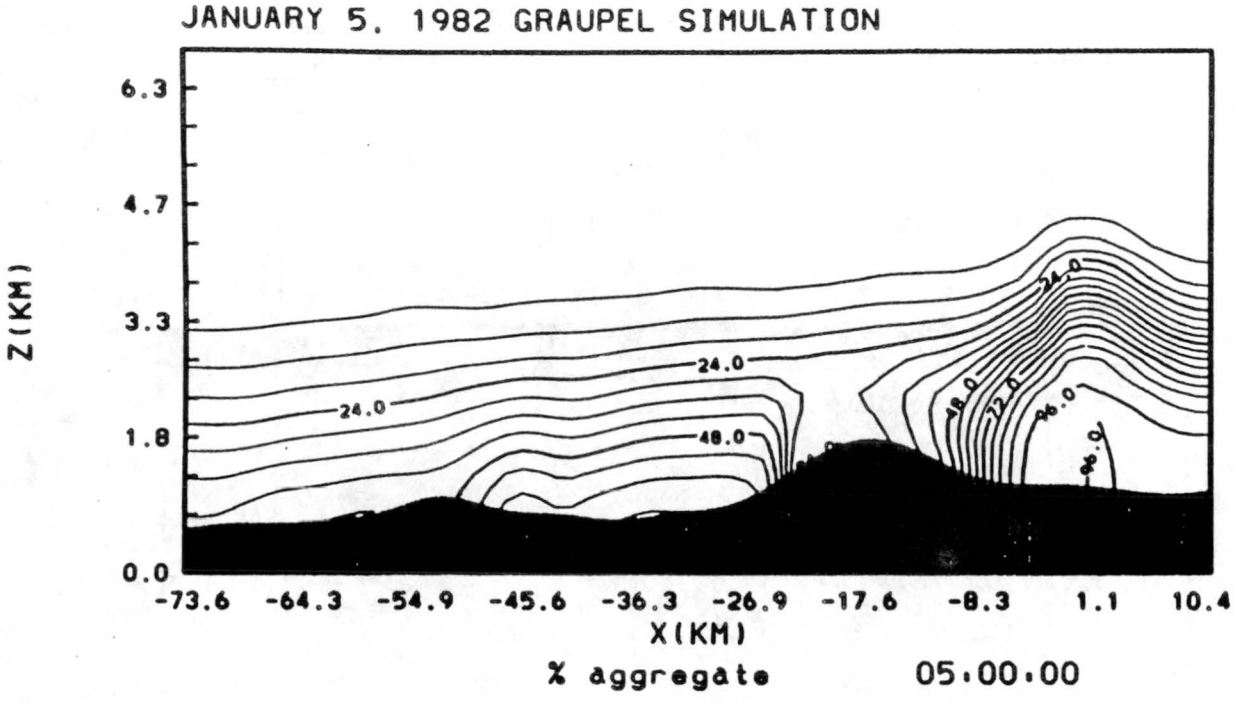

Figure 23. Mixing ratio of aggregates contoured over the smoothed COSE topography in intervals of 0.01 g/kg for the 5 January 1982 Graupel Experiment.

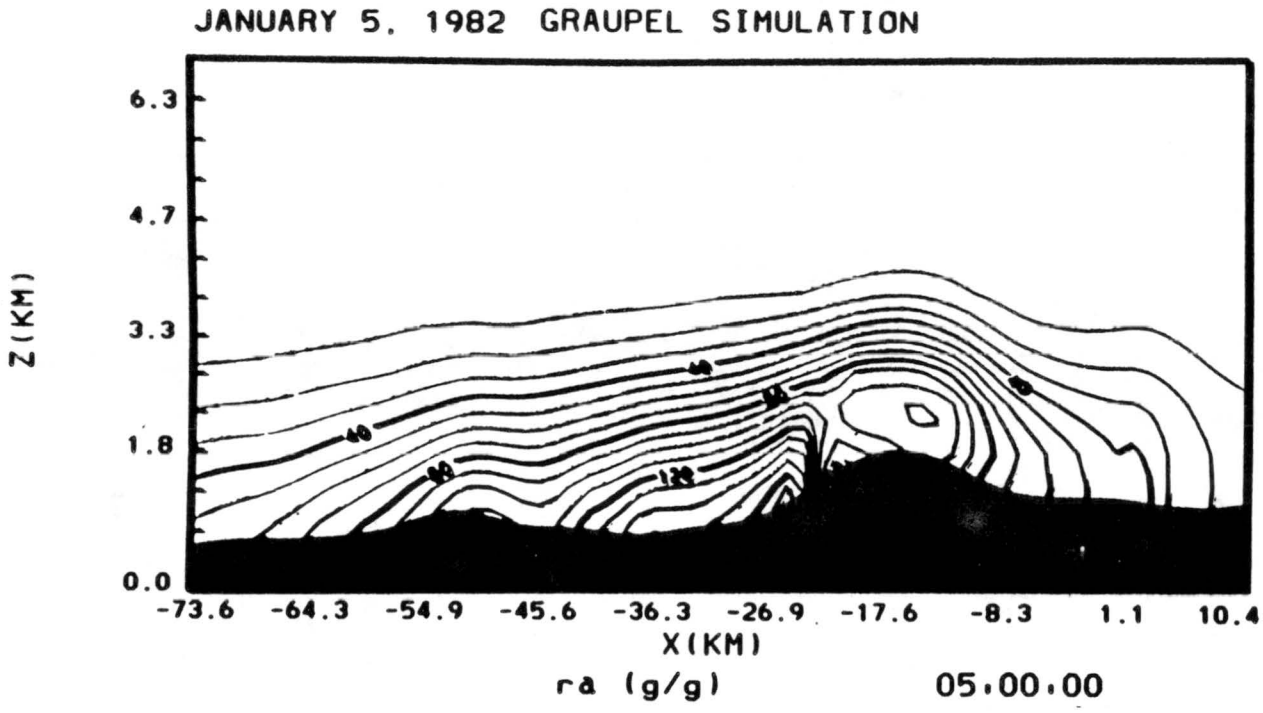

Figure 24. Percentage of precipitation predicted to be aggregates contoured over the smoothed COSE topography in intervals of 6 % for the 5 January 1982 Graupel Experiment.

smaller crystals (0.5 to 1.0 mm in diameter) had higher densities of 0.45 to 0.70 g/cm^3 exited while larger particles (1.0 to 2.0 mm) had densities of 0.25 to 0.45 g/cm^3. Based on these findings, two experiments were run. The first used a graupel density of 0.2 g/cm^3, and the second used a graupel density of 0.4 g/cm^3. These two values were chosen because of the variety of the observed values reviewed.

i. 21 December 1981: Graupel Density of 0.2

Graupel mixing ratios were greater (figure 25). The amount of increase varies in that well upwind of the barrier an increase of three times the control value was seen. Mixing ratios were nearly the same at -50 km and twice as high as the control on the lee side of the barrier. Since graupel was not predicted in the control experiment, an increase in the amount of graupel brings the simulation closer to that observed in the field.

Looking at the same figure, the cloud boundary is seen to be identical to the graupel experiment. Cloud water mixing ratios (figure 26) decreased over the barrier by 20%. Also, a decrease was seen upwind in the mid levels of the cloud. Little change was seen in the far western portion of the cloud. Cloud water was still not predicted in the areas detected during the aircraft flight.

Figure 27 shows the aggregate mixing ratios were reduced upwind of the barrier to one quarter of the graupel experiment predictions. Similar amounts were seen near the ground along the upwind slope of the barrier. On the lee side, mixing ratios were reduced by one eighth. The percent aggregates was found to decrease in the middle levels of the predicted

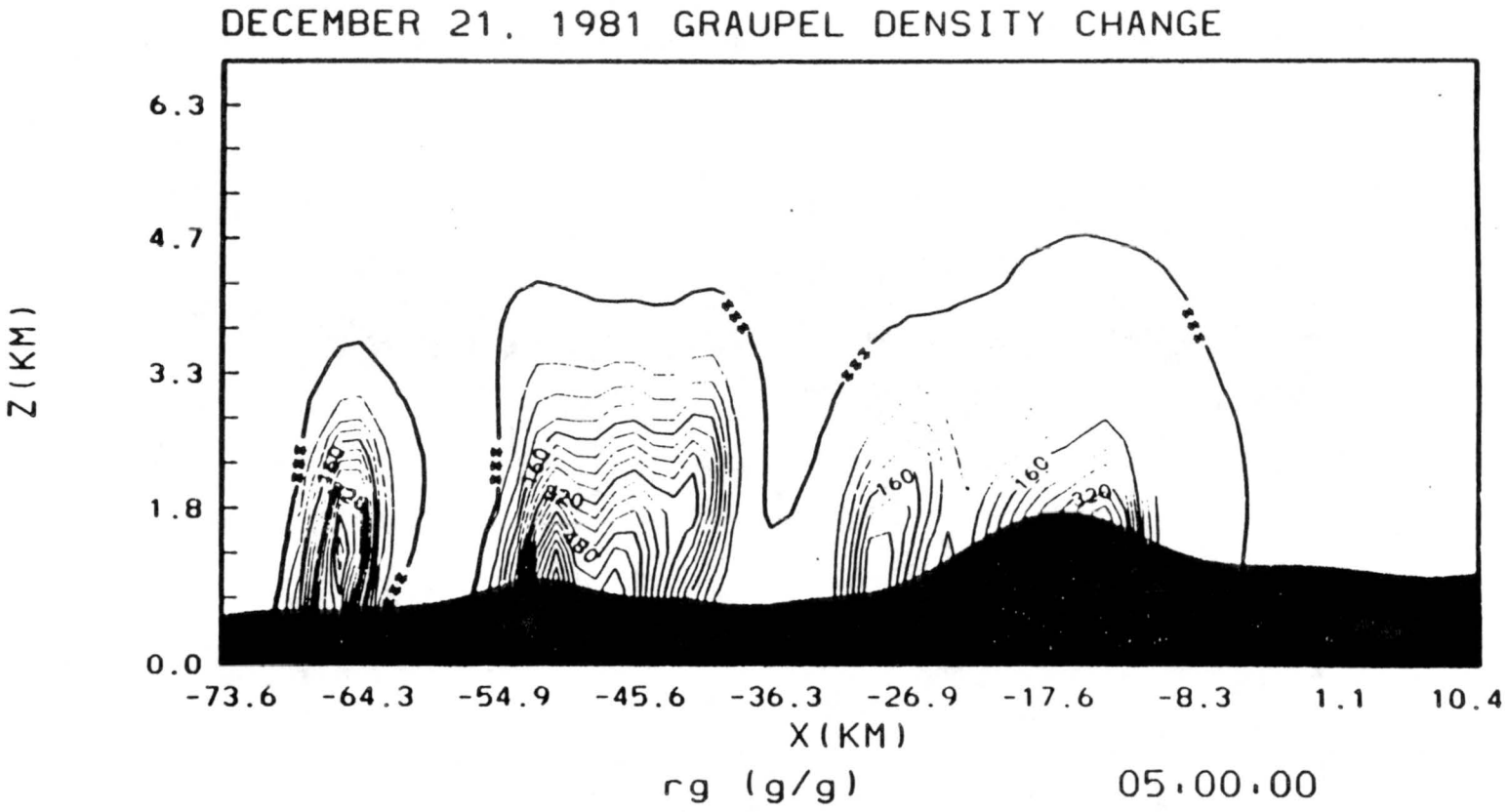

Figure 25. Mixing ratio of graupel contoured over the smoothed COSE topography in intervals of 0.004 g/kg for the 21 December 1981 Graupel Density Change to 0.2 g/cm^3 Experiment.

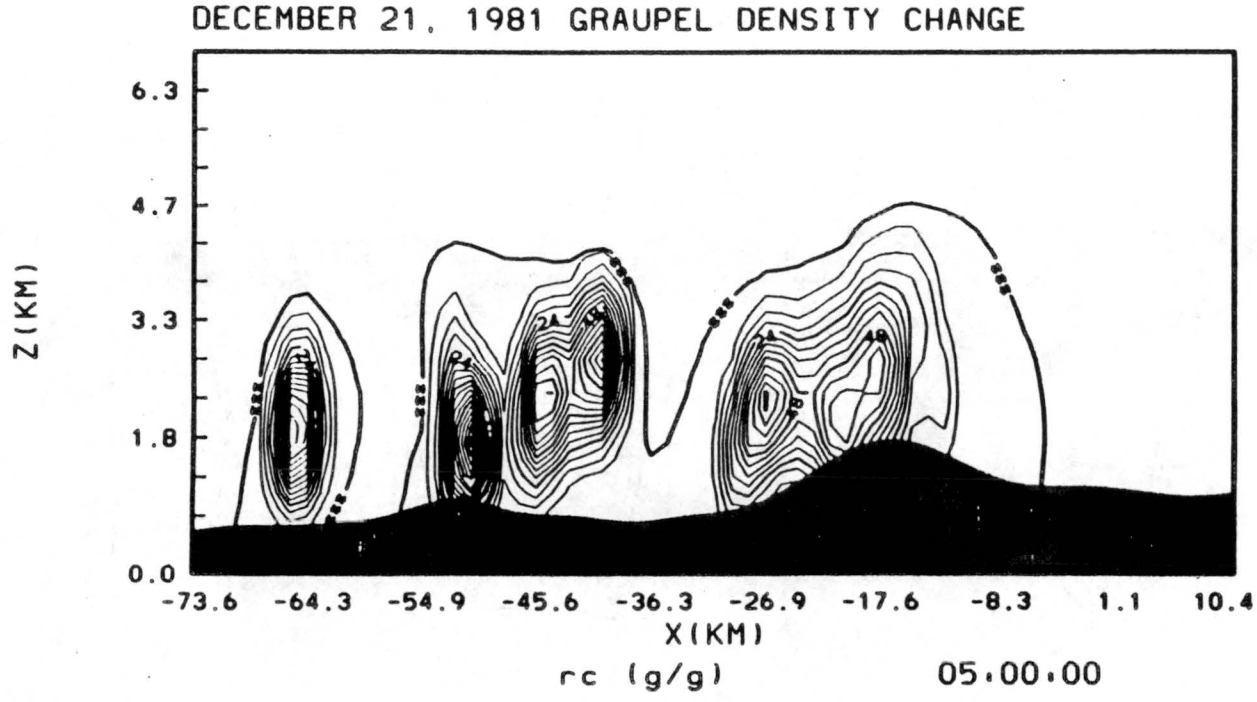

Figure 26. Mixing ratio of cloud water contoured over the smoothed COSE topography in intervals of 0.006 g/kg for the 21 December 1981 Graupel Density Change to 0.2 g/cm^3 Experiment.

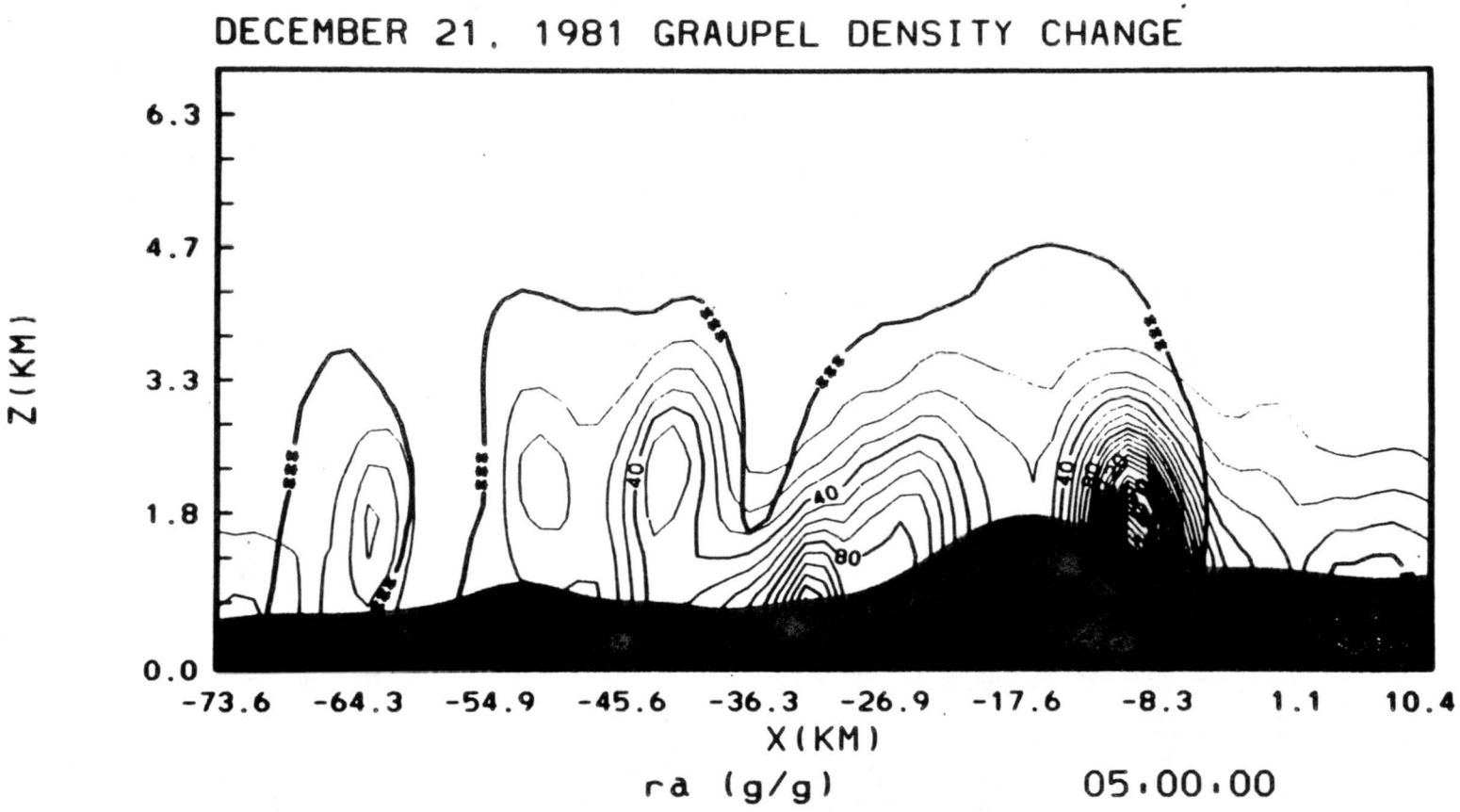

Figure 27. Mixing ratio of aggregates contoured over the smoothed COSE topography in intervals of 0.001 g/kg for the 21 December 1981 Graupel Density Change to 0.2 g/cm^3 Experiment.

clouds in areas where the largest decrease seen in the aggregate mixing ratio plots as seen in figure 28.

Comparing this to the graupel experiment, a larger increase was seen in the graupel mixing ratios while aggregate and cloud water mixing ratios showed a decrease.

ii. 21 December 1981: Graupel Density of 0.4

Little change was seen between this experiment and the change of density to 0.2 g/cm^3. The mixing ratio of graupel reduced to half the magnitude of the 0.2 experiment above -65 km in the x direction (figure 29). The other predicted quantities did not change over the 0.2 values. As can be seen in equation 17, the collection of cloud water by graupel is inversely proportional to the cubic root of the graupel density. The increase in graupel mixing ratio is thus greater for the lower density value. Theoretically, particles of lower density would fall at a slower rate (equation 16) allowing a greater collection of water droplets and thus a greater mass of graupel.

iii. 5 January 1982: Graupel Density of 0.2

On the western slope of the barrier, cloud water mixing ratios lowered only slightly over the graupel experiment. The graupel distribution and mixing ratio values are similar to the graupel experiment.

The distribution of aggregates remained the same as for the graupel simulation. Aggregate mixing ratios were also seen to remain the same.

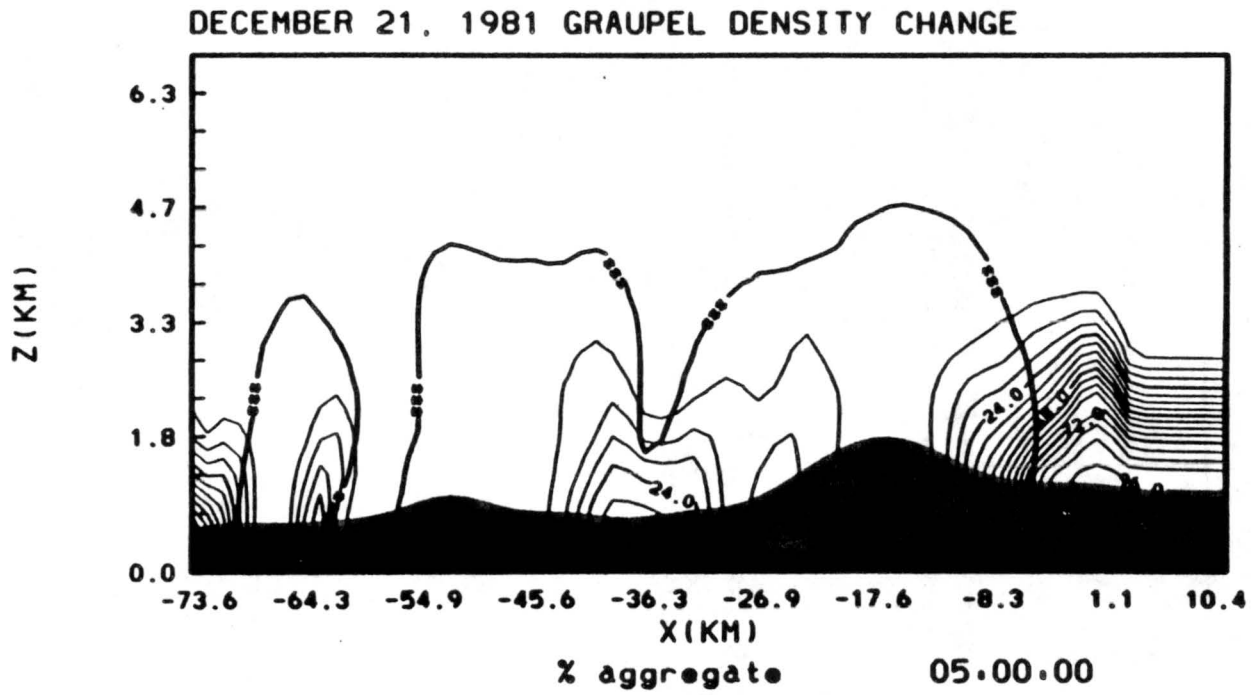

Figure 28. Percentage of precipitation predicted to be aggregates contoured over the smoothed COSE topography in intervals of 6 % for the 21 December 1981 Graupel Density Change to 0.2 g/cm^3 Experiment.

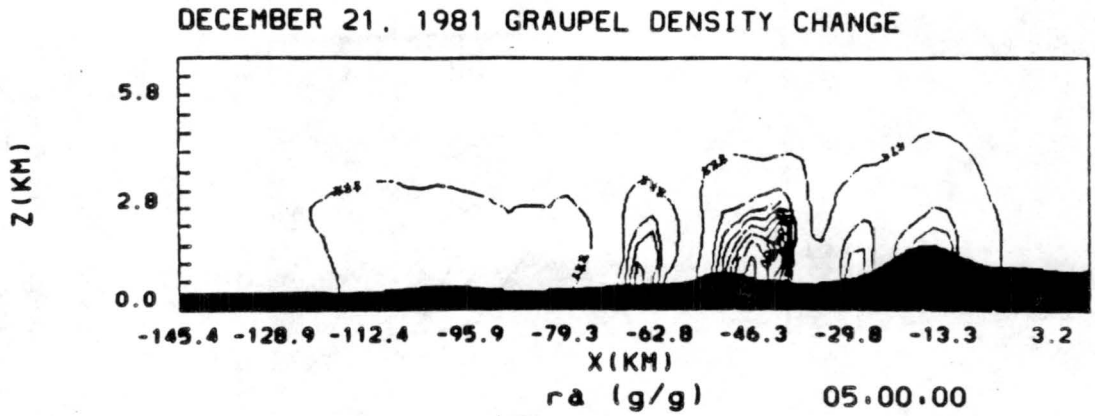

Figure 29. Mixing ratio of graupel contoured over the smoothed COSE topography in intervals of 0.008 g/kg for the 21 December 1981 Graupel Density Change to 0.4 g/cm^3 Experiment.

The percent of precipitation in the form of aggregates showed the same types of changes as with the graupel experiment.

iv. 5 January 1982: Graupel Density of 0.4

Cloud water mixing ratios increased by 0.002 g/kg over the 0.2 experiment. Overall, the mixing ratio of cloud water was between the graupel experiment and the 0.2 density experiment. Graupel mixing ratios were predicted to be nearly the same both in terms of distribution and magnitude. A slight increase in the mixing ratio of aggregates over the crest and lee slope of the barrier was predicted.

6.3 N_i Density Dependence Experiment

Ice crystals are predicted using a modified Fletcher curve as described in Chapter 3. There is no dependence on air density in this equation, so this experiment adds such a dependence. Since air density decreases with height, it should reduce the number of crystals predicted in the upper levels of the cloud.

i. 5 January 1982: N_i Density Dependence

The concentration of ice crystals was slightly reduced (figure 30). The predictions were not reduced to the degree necessary to solve the problem of overprediction at higher levels of the cloud. The model still simulated an increase in ice crystal concentration with height in the

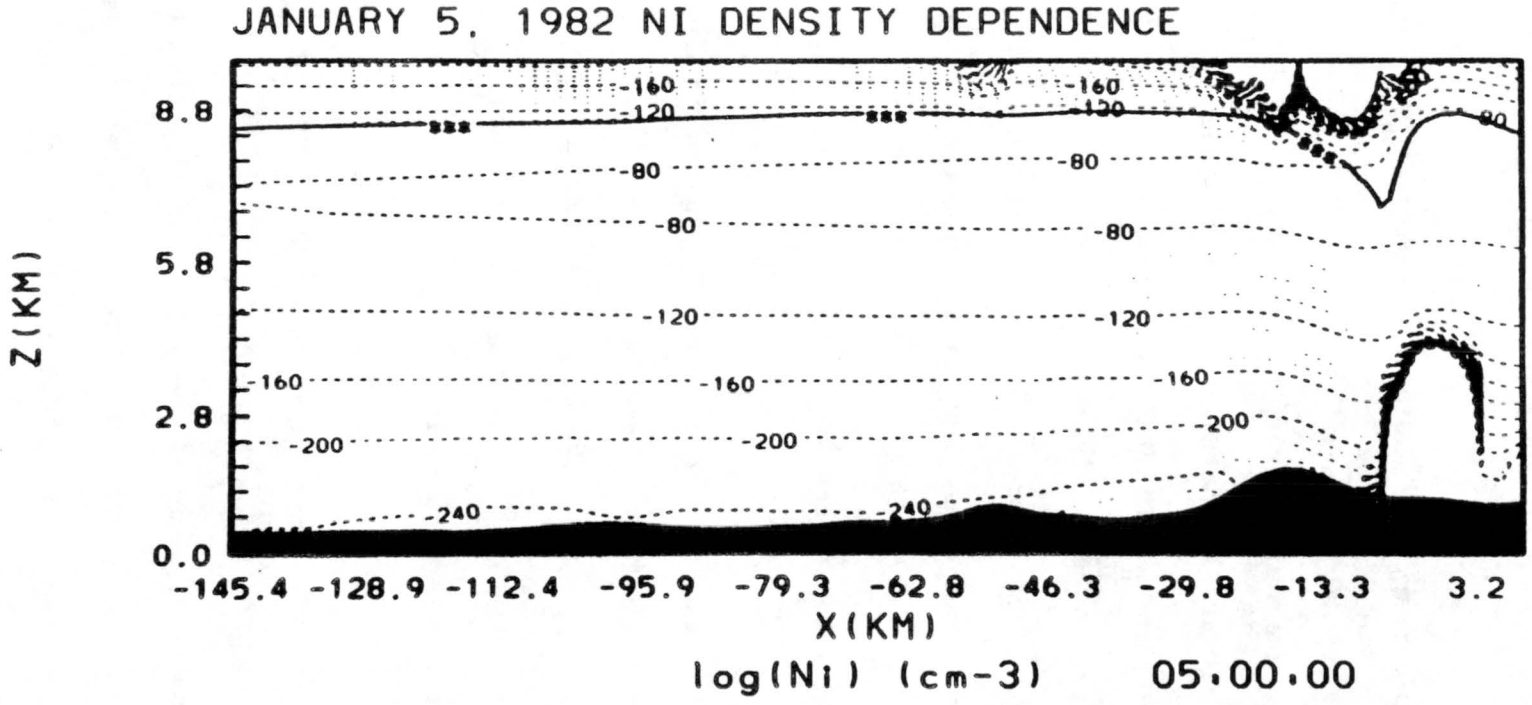

Figure 30. Logarithm of ice crystal concentration contoured over the smoothed COSE topography in intervals of 0.1 for the 5 January 1982 N_i Density Dependence Experiment.

cloud while observations showed a decrease of ice crystal concentrations with height.

The mixing ratio of cloud water (figure 31) increased by one fourth on the windward slope of the barrier with similar values over North Park. The mixing ratio of graupel was reduced by an order of magnitude (figure 32).

ii. 21 December 1981: N_i Density Dependence

The results of this experiment were similar to that of the aggregation case. Very little effect was seen in the concentration of ice crystals. The same problem of the concentration increasing with height occurred. The density dependence of the crystal concentration did not cure the problem.

6.4 Longwave Radiation Experiment

The radiation experiment evolved after the previous experiments had been analyzed. Longwave radiation was activated in the model to test the effects of radiational cooling. This experiment was run on the 21 December 1981 case to produce the liquid water near the top of the cloud which was observed during COSE. The production of the liquid water would be attributed to the radiational cooling at the top of the cloud. Since adjustments needed to be made to the model to run this experiment, the control experiment used in this study is not valid for detailed comparisons. The results of this experiment were as an initial exploratory sensitivity test.

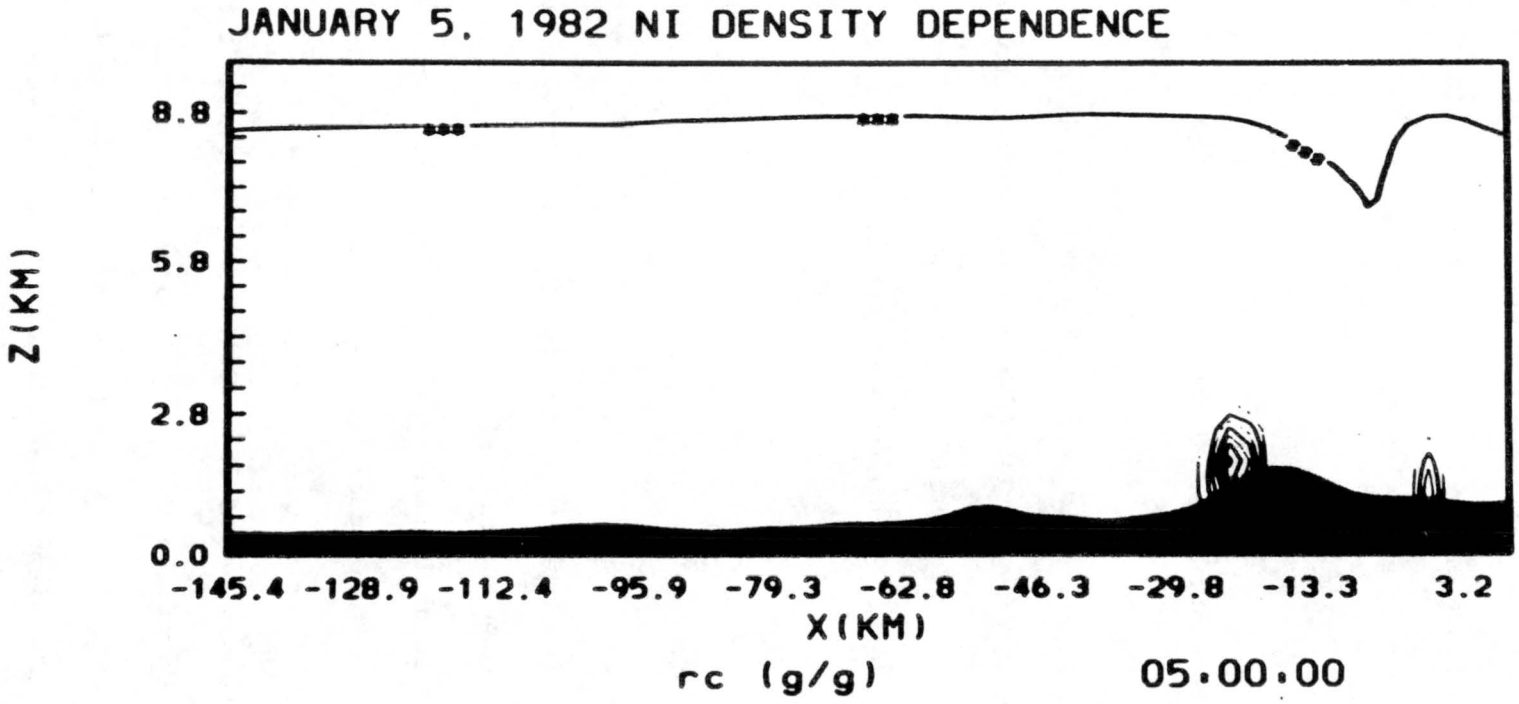

Figure 31. Mixing ratio of cloud water contoured over the smoothed COSE topography in intervals of 0.002 g/kg for the 5 January 1982 N_i Density Dependence Experiment.

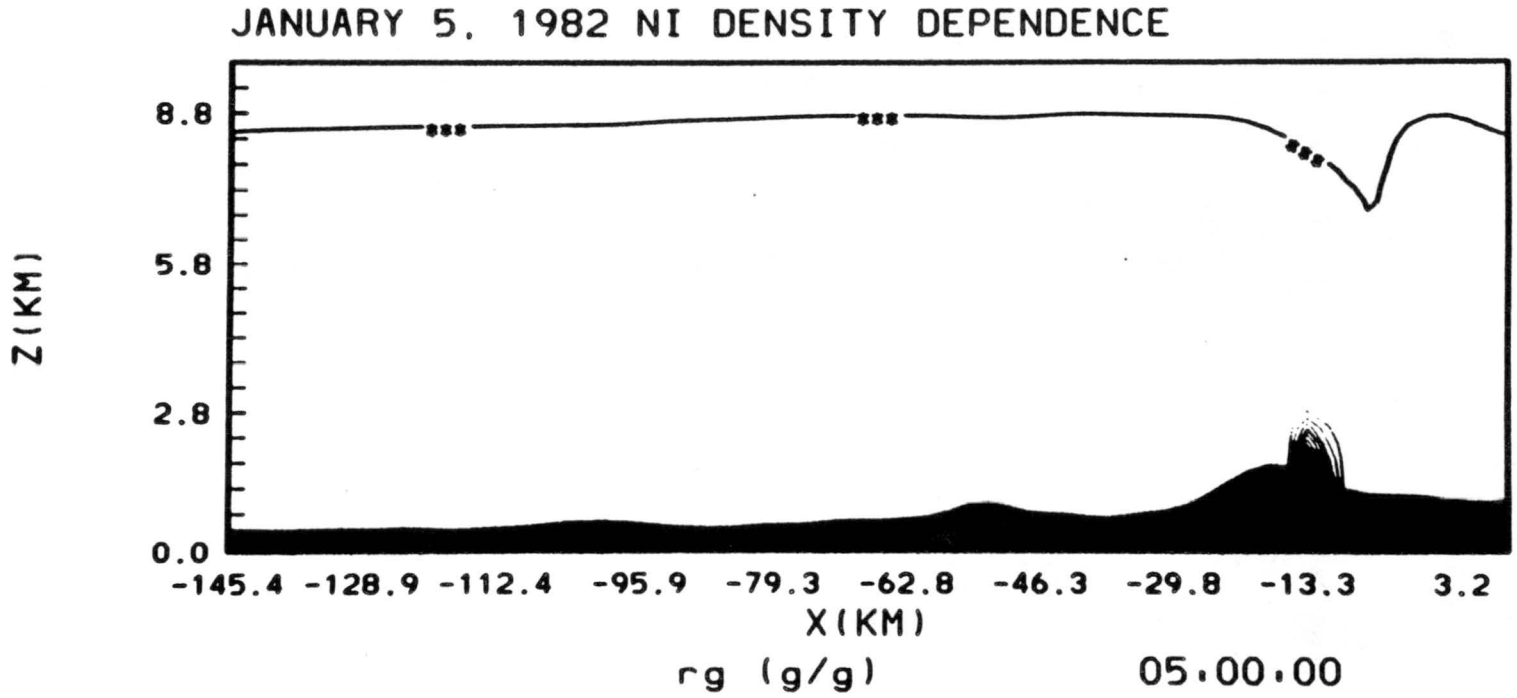

Figure 32. Mixing ratio of graupel contoured over the smoothed COSE topography in intervals of 0.00007 g/kg for the 5 January 1982 N_i Density Dependence Experiment.

The main differences were seen in the cloud boundary. A very smooth cloud top was predicted. Over the Park Range, mixing ratios of cloud water doubled, but no cloud water was predicted near the cloud top. The ice crystal concentrations were similar over the Park Range but doubled over the Front Range. The mixing ratio of aggregates also increased significantly. These results indicate further research is warranted.

Chapter 7. CONCLUSIONS

This study involved the analysis of the predictive capability of a mesoscale cloud model using field data from well documented winter orographic storms. Discrepancies found during numerical simulations were used to develop sensitivity tests and experiments. From the results of these experiments conclusions are made about model weaknesses and suggestions for further investigation follow.

The original numerical simulations (controls) consisted of a riming case and an aggregation case. The riming case used data from 21 December 1981. The model consistently predicted less liquid water than was observed by up to one half the observed values. At many places in the cloud, where aircraft observations indicated the presence of liquid water, none was predicted. The majority of the cloud water was predicted at levels below the flight path, thus making comparisons more difficult. A ground level comparison made indicated the mixing ratio of cloud water was underpredicted in the lower levels as well. The cloud boundary predicted showed distinct cells rather than a horizontal homogeneous top. This case may not have been the ideal control in that the cloud did not reach the steady state necessary for the comparisons made.

Cloud water is predicted using a constant droplet concentration of 60 cm^{-3}. For the liquid water contents predicted in these cases, the average cloud droplet radius would range between 7.5 μm and 3.5 μm. These

values are close to the threshold diameter for riming of 10 μm found by Borys et al. (1987). A better representation of droplet sizes would include a prediction of droplet concentrations. Also, the droplet size spectra should be included along with collection efficiencies based on droplet size. A threshold for riming would also improve the prediction of the riming process.

The aggregation case study used data collected on 5 January 1982. Since aggregation dominated the precipitation characteristics, much less liquid water was observed during this storm than in the riming case. Still, the model underpredicted observed liquid water contents. The same problem arose in that the majority of the cloud water predicted was below the flight path. The cloud boundary predicted for the aggregation case was much more uniform than in the riming case.

The effects of the radiation experiment on the mixing ratios of cloud water and aggregates as well as the ice crystal concentrations proved that the addition of longwave radiation into the model may be indicated.

Ice crystal concentrations predicted in the riming case study increased with height. Aircraft observations indicated a decrease in the crystal concentrations with height. At the highest levels of the cloud, the observed and predicted values were similar. Values at middle and lower levels differed by an order of magnitude.

The aggregation control simulation had the same discrepancy. In upper levels of the cloud, predicted ice crystal concentrations were twice the observed value. At lower levels of the cloud predicted values were one half the observed values.

Graupel was not predicted in the riming control simulation though heavy rime was observed on crystals at the ground. In the aggregation case graupel was predicted in low values where no observations were made. The main reason for the lack of graupel predicted was the high graupel density value of 0.6 g/cm^3 used in the model.

The distribution of aggregates was predicted correctly in both control simulations. The percentage of aggregates predicted was underestimated in the aggregation simulation.

The basic discrepancies found from the control simulations include all of the quantities observed. Cloud water was underpredicted. The vertical distribution of ice crystal concentrations predicted was opposite of that observed. Graupel was not predicted with the case that riming dominated and aggregates were underpredicted in the aggregation case.

The experiments conducted included modification to the graupel and the ice crystal parameterizations. The other quantities were examined in terms of how the changes affected the predicted values.

The first simulation, labeled the Graupel Experiment, removed the threshold for graupel to form. The experiment run on the riming case produced graupel. This was an improvement over the control simulation in which no graupel was predicted. The cloud boundary showed a distinct change and cloud water increased over the barrier. Cloud water was still not predicted where it was observed by the aircraft. Ice crystal concentrations were predicted in lower concentrations causing a greater difference compared to the observed values. Aggregates were seen to decrease.

The graupel experiment run on the 5 January 1982 data showed a decrease in graupel on the leeside of the barrier. The graupel

distribution was seen to shift to the west. Cloud water increased on the leeside where the graupel concentration decreased. Aggregates were reduced where the graupel was predicted which caused a greater underprediction of the percentage of the precipitation which fell in the form of graupel.

The second set of experiments involved decreasing the graupel density to 0.2 g/cm^3 and 0.4 g/cm^3. For the 21 December 1981 case, Graupel was greatly increased and both the cloud water and aggregates were reduced. This made the predicted characteristics closer to the observed. The main difference between the two different densities was that more graupel was predicted in the 0.2 g/cm^3. The amount of graupel predicted by the model is inversely proportional to the cubic root of the graupel density.

The graupel density experiments had little effect on the aggregation case. Cloud water decreased slightly and there was a slight increase in the amount of aggregates. Since only and isolated area of graupel was predicted in the control simulation, these results should be expected.

The last set of experiments addresses the problem with the prediction of ice crystals. The aggregation case showed only a slight reduction in the ice crystal concentrations in the upper levels of the clouds and the vertical distribution was not reversed as observed by the aircraft. Cloud water increased on the leeside of the barrier where the graupel mixing ratios decreased. The riming case showed little effect.

These experiments show that a decrease in the graupel density used in the microphysical parameterization of the model is indicated. The original value of 0.6 g/cm^3 was based on convective cloud systems and is not appropriate for these cold, stable orographic clouds.

The problem of the ice crystal concentrations was not easily solved. As mentioned in Chapter 5, the reason for the discrepancy between predicted and observed values may be due to boundary layer effects. Though Steamboat Springs is a relatively pristine area, the low level concentrations of ice nuclei may be distinctly different than the upper level air which has been highly modified. This idea is further addressed in the next chapter.

Also, comparisons of model output with field data are extremely limited in that the model gives values over the whole domain while field observations are limited to selected locations.

Suggestions can be made to improve the model. A decrease in the graupel density used is indicated. The value of 0.2 g/cm^3 worked best for the riming case simulated. This agrees with values measured in field experiments. The introduction of air density into the crystal concentration equation yielded positive results though did not solve all the discrepancies observed in the predicted ice crystal concentrations. Further research is indicated.

Chapter 8. AREAS FOR FUTURE RESEARCH

Precipitation observed at ground level gives a signature of the cloud from which it originated. The characteristics of the precipitation imply crystal concentrations, size and distribution, liquid water content, droplet size and to some extent cloud dynamics. Understanding the microphysical processes involved in the development of precipitation size particles, helps increase the understanding of precipitation events and the ultimate forecasting of them.

Orographic clouds can provide a reasonably steady state system in which to study cloud and precipitation microphysics. Conclusions made during orographic studies can be extrapolated to convective clouds. Aggregation and riming, both important mechanisms in the growth of precipitation size particles, are more easily studied in stratiform clouds.

This study raises several ideas for further development and testing of microphysical representations in mesoscale cloud models. Inadequacies in the present configuration of the model include grid spacing, ice crystal production and most importantly comparison limitations between field observations and model predictions.

The domain necessary to achieve a realistic air flow model requires a much larger grid spacing than the scale on which microphysical processes operate. There is no easy solution to this problem, but a smaller grid spacing in the area of interest (i.e,, along the barrier slope) could give

greater detail of the storm system to aid in comparisons with field data. Since it is impossible to run a mesoscale model with microscale grid spacing, a compromise must be made. Thus the advantages of a steady state orographic cloud become obvious. A much larger grid spacing can be used while still representing the cloud with some accuracy. Since the microphysical characteristics of the cloud vary more vertically than horizontally, a smaller vertical grid spacing is necessary. In fact, the smallest possible vertical grid spacing should be used. The 500 m spacing used in these experiments was too large. A rerun of these experiments with smaller spacing is indicated.

The experiments dealing with ice crystal concentration brought out a discrepancy well worth further investigation. The problem with predicted crystal concentration increasing with height while observed crystal concentrations decreased with height. Both Cotton et al. (1986) and Blumenstein et al. (1982) discussed this occurrence. The effects of boundary layer air versus more pristine air at upper levels acts to contradict the temperature dependent method used by the model. A modification of the lower layers of the model could include boundary layer type concentrations of IN while upper layers showed smaller concentrations.

The exploratory sensitivity experiment which introduced longwave radiation into the model yielded interesting results worth futher investigation.

The largest problem which arose in this experiment was in comparing model output with field observations. Future field studies should be developed to facilitate such comparisons. The main area which needs to be expanded is measurements near cloud base. These were not possible

because of aircraft limitations during the project. The data which was most helpful was taken during spirals made by the aircraft over the radar site. Observations were made of an entire column through the cloud over a short period of time which could be compared with radar and radiometer data. Spirals to greater depths, proposed but not approved for the latest COSE, would be ideal.

The problem, of the detail of field observations should also be addressed. Since observations cannot be made in great detail over the whole domain, more detailed analysis of model results in the observation areas should be developed. Comparisons at specific points could then be made.

Using field data for the analysis of numerical models allows the type of testing necessary to develop a realistic model. There is much future study possible in this type of modeling.

Chapter 9. REFERENCES

Blumenstein, R.R., R.M. Rauber and L.O. Grant, 1982: Microphysical growth processes during a rapidly evolving orographic cloud system. Proceedings, Conf. on Cloud Physics, AMS, Chicago, IL, 481-484.

Borys, R.D., E.E. Hindman and P.J. DeMott, 1987: The chemical fractionation of atmospheric aerosols as a result of snow crystal formation and growth. J. Atmos. Chem.,

Chang, C.H., 1977: Ice generation in clouds. M.S. thesis, Dept. Meteor., South Dakota School of Mines and Technology, Rapid City, SD, 129 pp.

Cooper, W.A. and G. Vali, 1981: the origin of ice in mountain cap clouds. J. Atmos. Sci., 38, 1244-1259.

Cotton, W.R., E.A. Mulvihill, G.J. Tripoli and R.M. Rauber, 1985: The simulation of orographic snowfall over the northern Colorado Rockies---A blind simulation experiment. Proceedings, Fourth WMO Sci. Conf. on Weather Modification, Honolulu, HI, 147-148.

Cotton, W.R., M.A. Stephens, T. Nehrkorn and G.J. Tripoli, 1982: The Colorado State University three-dimensional cloud/mesoscale model--1982. Part II: An ice phase parameterization. J. de Rech. Atmos., 16, 295-320.

Cotton, W.R., G.J. Tripoli, R.M. Rauber and E.A. Mulvihill, 1986: Numerical simulation of the effects of varying ice crystal nucleation rates and aggregation processes on orographic snowfall. J. Clim. Appl. Meteor., 25, 1658-1680.

D'Errico, R.E. and A.H. Auer, 1978: An observational study of the riming properties of ice crystals of simple geometric shapes. Preprints Conf. Cloud Physics and Atmos. Electricity, Issaquah, AMS, 114-121.

Fletcher, N.H., 1968: Surface structure of water and ice, II-a revised model. Phil. Mag., 18, 1287-1300.

Grant, L.O., P.J. DeMott and R.M. Rauber, 1982: an inventory of ice crystal concentrations in a series of stable orographic cloud systems. Proceedings, Conf. on Cloud Physics, AMS, Chicago, IL, 584-587.

Hariyama, T., 1975: The riming properties of snow crystals. J. Meteor. Soc. Japan, 53, 384-392.

Heymsfield, A.J., 1967: Snow crystal types observed in snow squalls. Internal Publ. State University of New York, Fredonia, 12 pp.

Heymsfield, A.J., 1982: A comparative study of the rates of development of potential graupel hail embryos in high plains storms. J. Atmos. Sci., 39, 2867-2897.

Hindman, E.E., R.D. Borys and P.J. DeMott, 1983: Hydrometeorological significance of rime ice deposits in the Colorado Rockies. Water Res. Bull., 19, 619-624.

Hobbs, P.V., S. Chang and J.D. Locatelli, 1974: The dimensions and aggregation of ice crystals in natural clouds. J. Geophys. Res., 79, 15, 2199-2206.

Hobbs, P.V., R.C. Easter and A.B. Fraser, 1973: A theoretical study of the flow of air and fallout of solid precipitation over mountainous terrain, Part II: Microphysics. J. Atmos. Sci., 30, 813-823.

Hobbs, P.V. and B.J. Mason, 1964: The sintering and adhesion of ice. Phil. Mag., 9, 181-197.

Hobbs, P.V., L.F. Radke, A.B. Fraser, J.D. Locatelli, C.E. Robertson, D.G. Atkinson, R.J. Farber, R.R. Weiss and R.C. Easter, 1971: Studies of winter cyclonic storms over the Cascade Mountains (1970-71). Res. Rept. VI, Cloud Physics Group, University of Washington, 306 pp.

Hogg, D.C., F.O. Guiraud, J.B. Snider, M.T. Decker and E.R. Westwater, 1983: A steerable dual-channel microwave radiometer for measurement of water vapor and liquid in the troposphere. J. Clim. Appl. Meteor., 22, 789-806.

Holroyd, E.W., III, 1964: A suggested origin of conical graupel. J. Appl. Meteor., 3, 633-636.

Hosler, C.L., D.C. Jensen and L. Goldshlak, 1957: On the aggregation of ice crystals to form snow. J. Meteor., 14, 415-420.

Hosler, C.L. and R.E. Hallgren, 1960: The aggregation of small ice crystals. Disc. Farad. Soc., 30, 200-208.

Huffman, P.J. and G. Vali, 1973: The effect of vapor depletion on ice nucleus measurements with membrane filters. J. Appl. Meteor., 12, 1018-1024.

Jiusto, J.E., 1971: Crystal Development and glaciation in a supercooled cloud. J. Rech. Atmos., 55, 69-85.

Jiusto, J.E. and M.L. Kaplan, 1972: Snowfall from lake effect snowstorms. Mon. Wea. Rev., 100, 62-66.

Jiusto, J.E. and H.K. Weickmann, 1973: Types of snowfall. Bull. Amer. Meteor. Soc., 54, 1148-1162.

Knight, C.A. and N.C. Knight, 1970: Hail stone embryos. J. Atmos. Sci., 27, 659-666.

Knight, C.A. and N.C. Knight, 1973: Conical graupel. J. Atmos. Sci., 30, 118-124.

Lin, Y-L., R.D. Farley and H.D. Orville, 1983: Bulk parameterization of the snow field in a cloud model. J. Clim. Appl. Meteor., 22, 1065-1092.

Latham, J. and C.P.R. Saunders, 1971: Experimental measurements of the collection efficiencies of ice crystals in electric fields. Quart. J. Roy. Meteor. Soc., 96, 257-265.

Magono, C. and C.W. Lee, 1966: Meteorological classification of natural snow crystals. J. Fac. Sci., Hokkaido Univ. Ser. 7, 2, 321-362.

Magono, C. and S. Tazawa, 1972: Aggregation phenomena of ice crystals. J. Meteor. Soc. Japan, Series II, 50(5), 489-493.

Mulvihill, E.A., L.O. Grant, W.R. Cotton and G.J. Tripoli, 1986: Riming characteristics of orographic clouds in the Colorado Rockies. Proceedings, Conf. on Cloud Physics, AMS, Snowmass, CO, 231-232.

Mulvihill, E.A., G.J. Tripoli, L.O. Grant and W.R. Cotton, 1986: A review of aggregation parameterizations in modeling. Proceedings, Tenth Conf. on Weather Modification, AMS, Arlington, VA, 156-158.

Odencrantz, F.K., W.S. McEwan, P. St.Amand and W.G. Finnegan, 1968: Mechanism for multiplication of atmospheric ice crystals. Science, 160, 1345-1346.

Ohtake, T., 1969: Factors affecting the size distribution of raindrops and snowflakes. J. Atmos. Sci., 27, 804-813.

Ono, A., 1969: The shape and riming properties of ice crystals in natural clouds. J. Atoms. Sci., 26, 138-147.

Passarelli, R.E., and R.C. Srivastava, 1979: A new aspect of snowflake aggregation theory. J. Atmos. Sci., 36, 484-493.

Pitter, R.L., 1977: A reexamination of riming on thin ice plates. J. Atmos. Sci., 34, 684-685.

Prupacher, H.R. and J.D. Klett, 1978: Microphysics of Clouds and Precipitation, Reidel, 714 pp.

Power, B.A., P.W. Summers and J. D'Avignon, 1964: Snow crystal forms and riming effects as related to snowfall density and general storm conditions. J. Atmos. Sci., 21, 300-305.

Rauber, R.M., 1985: Physical Structure of Northern Colorado River Basin cloud systems. Atmos. Sci. Paper #390, Dept. Atmos. Sci., Colorado State University, Fort Collins, CO, 362 pp.

Rauber, R.M., L.O. Grant and J.B. Snider, 1982: Spatial and temporal variations of cloud liquid water determined by aircraft and microwave radiometer measurements in northern Colorado orographic storms. Proceedings, Conf. on Cloud Physics, AMS, Chicago, IL, 477-480.

Reinking, R.F., 1973: Empirical assessment of riming microphysics. Ph.D. dissertation, Colorado State University, Fort Collins, CO, 342 pp.

Reinking, R.F., 1975: Formation of graupel. J. Appl. Meteor., 14, 745-754.

Reinking, R.F., 1979: The onset and early growth of snow crystals by riming of droplets. J. Atmos. Sci., 36, 870-881.

Rogers, D.C., 1974: The aggregation of natural ice crystals. M.S. Thesis, Dept of Atmos. Research, University of Wyoming, Laramie, WY, 87 pp.

Rogers, D.C., D. Baumgardner and G. Vali, 1983: Determination of supercooled liquid water content by measuring rime rate. J. Clim. Appl. Meteor., 22, 153-162.

Sasyo, Y., 1971: Study of the formation of precipitation by aggregation of snow particles the riming of cloud droplets on snowflakes. Papers Meteor. Geophys., 22, 69-142.

Smith-Johannsen, R.I., 1965: Resin vapour replication technique for snow crystals and biological specimens. Nature, 205, 1204-1205.

Smith-Johannsen, R.I., 1969: Ice crystal agglomeration: T-Formation. J. Atmos. Sci., 26, 532-534.

Uttal, T., 1985: Distribution of liquid, vapor and ice in a phase budget of a Colorado orographic cloud system. M.S. Thesis, Colorado State University, Fort Collins, CO, 97 pp.

Wilkins, R.I. and A.H. Auer, 1970: Riming properties of hexagonal ice crystals. Preprints Conf. Cloud Physics, Fort Collins, CO, AMS, 81-82.

Young, K.C., 1974a: A numerical simulation of wintertime, orographic precipitation: Part I. Description of model microphysics and numerical techniques. J. Atmos. Sci., 31, 1735-1748.

Young, K.C., 1974b: A numerical simulation of wintertime, orographic precipitation: Part II. Comparison of natural and AgI-seeded conditions. J. Atmos. Sci., 31, 1735-1748.